

Tire/road friction estimation for front wheel driven vehicle

Simon Johansson

Viking Persson



LUND
UNIVERSITY

Department of Automatic Control

MSc Thesis
ISRN LUTFD2/TFRT--5985--SE
ISSN 0280-5316

Department of Automatic Control
Lund University
Box 118
SE-221 00 LUND
Sweden

© 2015 by Simon Johansson & Viking Persson. All rights reserved.
Printed in Sweden by Tryckeriet i E-huset
Lund 2015

LUND UNIVERSITY

Abstract

Faculty of Engineering
Department of Automatic Control

Master of Science in Electrical Engineering

by

[Simon Johansson](#)

[Viking Persson](#)

Vehicles of today are equipped with several driving enhancing systems. The Electronic Stability Program (ESP) controls the brakes of the vehicle to prevent undesirable vehicle behavior. The Anti-lock Braking System (ABS) prevents the wheels to lock up while braking hard. Many vehicles are also equipped with advanced All Wheel Drive (AWD) systems or Limited Slip Differentials (LSD) allowing for the drive torque to be almost freely distributed among the wheels. Knowing the coefficient of friction to the road is extremely beneficial for all of these systems, especially for the AWD and LSD systems to be able to optimize the control.

In this master thesis a method for estimating the tire/road friction coefficient will be developed. Focus will be put on Front Wheel Driven (FWD) vehicles equipped with an electronic Limited Slip Differential (eLSD). The eLSD in question is a newly launched product by BorgWarner AB called FXD (Front Cross Differential). This is an eLSD based on their well known fifth generation electro hydraulic clutch. Today it's controlled by a complex control algorithm to be able to handle several driving situations. It's desirable to know the tire/road friction coefficient to improve the control algorithm further. This is especially important when estimating the torque transfer through the differential.

Acknowledgements

We would like to thank the following persons.

Ted Brink *Supervisor and mentor at BorgWarner TorqTransfer Systems AB in Landskrona*

Ola Nockhammar *Supervisor and mentor at BorgWarner TorqTransfer Systems AB in Landskrona*

Tore Hägglund *Supervisor and mentor at Department of Automatic Control, Faculty of Engineering, Lund University*

Anders Robertsson *Examiner at Department of Automatic Control, Faculty of Engineering, Lund University*

We would also like to thank BorgWarner TorqTransfer Systems AB in Landskrona with employees for lending us necessary equipment and aiding us with invaluable information to help us in our work.

Contents

Abstract	i
Acknowledgements	ii
Abbreviations	vi
Symbols	vii
1 Introduction	1
1.1 Background	1
1.2 Project goal	1
1.3 Volkswagen Golf GTi Mk7	2
2 Theory	3
2.1 Vehicle dynamics and models	3
2.1.1 The bicycle model	3
2.1.2 Two track vehicle model	6
2.1.3 Normal forces	7
2.1.3.1 Lateral load transfer	7
2.1.3.2 Longitudinal load transfer	8
2.1.3.3 Longitudinal and lateral load transfer combined	9
2.2 Tire dynamics	10
2.2.1 Longitudinal forces	11
2.2.2 Lateral forces	12
2.2.3 Combined slip	14
2.2.4 Tire stiffness	15
2.3 Tire models	15
2.3.1 Brush model	16
2.3.2 The Magic Formula tire model	17
2.3.3 Dugoff tire model	20
2.3.4 The BW tire model	20
2.4 Differentials	21
2.4.1 Open differential	21
2.4.2 Problems with the open differential	21
2.4.3 Limited slip differential	23

2.4.4	FXD	23
2.4.4.1	The clutch	23
2.4.4.2	The differential	24
2.4.4.3	Control algorithm	24
2.4.4.4	Benefits of the FXD	24
3	Friction	26
3.1	What is friction?	26
3.2	Tire/road friction	27
3.3	Downforce	28
4	Friction estimation method	29
4.1	Approach	29
4.1.1	Practical restrictions and problems	30
4.1.2	FXD	31
4.1.3	Related work	31
4.1.4	Conclusion	32
4.2	Signal processing	32
4.2.1	Filters	33
4.2.2	Static parameter impact	34
4.3	Vehicle forces	35
4.3.1	Vehicle force calculated from longitudinal acceleration	36
4.3.1.1	Estimating the longitudinal acceleration	36
4.3.1.2	Estimating the losses	37
4.3.1.3	Estimating the total vehicle force	37
4.3.1.4	Complications	37
4.3.2	Vehicle force calculated from engine torque	38
4.3.2.1	Gear ratio	40
4.3.2.2	Transfer losses	41
4.3.2.3	Complications	42
4.3.2.4	Verification	42
4.3.3	Choosing vehicle model	42
4.4	Tire forces	45
4.4.1	Choosing a tire model	46
4.4.2	Tire model parameters for the BW tire model	47
4.4.2.1	Tire stiffness	47
4.4.2.2	Slip ratio	48
4.4.2.3	Normal force	49
4.4.2.4	Friction coefficient	51
4.5	Fitting the tire model	51
4.5.1	Winter tires	52
4.5.2	Summer tires	55
4.5.3	Lateral acceleration compensation	56
4.5.4	Tire mode selector	58
4.6	Estimating the friction coefficient	60
4.6.1	Least square fitting	60
4.6.2	Recursive least square fitting	61

4.6.3	When to estimate the friction coefficient	62
4.6.3.1	Limitations due to slip ratio	62
4.6.3.2	Limitations due to gear shifts	64
4.6.3.3	Limitations due to low forces	64
5	Results	67
5.1	Tire/road friction for different driving sessions	67
5.1.1	Winter tires on asphalt	67
5.1.2	Winter tires on ice	69
5.1.3	Winter tires on asphalt and ice combined	70
5.1.4	Summer tires on asphalt	73
5.1.5	Summer tires on wet asphalt	74
6	Discussion	76
6.1	Modeling the forces	76
6.1.1	The complexity of a tire	76
6.1.2	Approximating the losses	77
6.1.3	Slip ratio calculations	77
6.1.4	Weight load transfer	78
6.2	Evaluating the results	78
6.2.1	Using winter tires	78
6.2.2	Using summer tires	79
7	Conclusion	81
7.1	Model parameters	81
7.2	CAN signals used	81
7.3	Final words	82
	Bibliography	83

Abbreviations

ABS	Anti-lock Brake System
AWD	All Wheel Driven
CAN	Controller Area Network
CoG	Center of Gravity
eLSD	electronic Limited Slip Differential
ESP	Electronic Stability Program
FWD	Front Wheel Driven
FXD	Front <i>Cross</i> Differential
LSD	Limited Slip Differential
RLS	Recursive Least Square
RWD	Rear Wheel Driven

Symbols

α	slip angle	rad
β	factor for lateral acceleration compensation	-
δ	steering angle	rad
η	efficiency factor	-
κ	slip ratio	-
λ	forgetting factor, RLS	-
ξ	tire parameter specific to the BW tire model	-
τ	factor for amount of used friction	-
μ	coefficient of friction	-
μ_0	normalized force ($\frac{F_x}{F_z}$)	-
$\dot{\psi}$	yaw rate	rads ⁻¹
ω	angular velocity	rads ⁻¹
C_x	longitudinal tire stiffness	-
C_y	lateral tire stiffness	-
F_{rr}	rolling resistance	N
F_x	longitudinal force	N
F_y	lateral force	N
F_z	normal force	N
l_f	distance between CoG and front axle	m
l_r	distance between CoG and rear axle	m
R_e	effective rolling radius	m
T_w	track width	m
V_x	longitudinal vehicle speed	ms ⁻¹
V_y	lateral vehicle speed	ms ⁻¹

Chapter 1

Introduction

1.1 Background

During the spring of 2013 BorgWarner AB went into production with their new product called Front Cross Differential (FXD). This is a brand new electronic Limited Slip Differential (eLSD) for front wheel driven cars which uses some of the technology from their well-known four-wheel-drive systems. Being able to control the applied torque on each wheel results in increased traction, better cornering performance and improved safety.

The torque control is done by a complex algorithm that uses several signals from the car. It has been shown that the tuning of this algorithm is different depending on tire stiffness and road condition. It is therefore desirable to extend the algorithm to be able to estimate tire stiffness and the tire/road friction coefficient.

1.2 Project goal

The goal of the project is to estimate the tire stiffness and the tire/road friction coefficient. The system needs to be fast and robust to be trusted in all conditions. Another constraint is to make an estimator that relies on signals easily available on the Controller Area Network (CAN) bus of the vehicle. It's supposed to work in a normal car and not only be restricted to testing in cars equipped with advanced technology to measure signals that are not normally available.

1.3 Volkswagen Golf GTi Mk7

The latest Golf GTi from Volkswagen is equipped with the FXD. All driving data used in this work have been collected with this kind of car. Borg Warner has one of these cars in Landskrona that has been driven to collect data. The car at Borg Warner is equipped with Volkswagen's DSG transmission which is an automatic transmission with the options to shift gear manually with paddles at the steering wheel. Whenever a car is referred to in the report, it is this Golf GTi, if nothing else is explicitly stated.



FIGURE 1.1: Golf GTi Mk7 equipped with FXD.

Chapter 2

Theory

Before describing the work on friction estimation it is important to have some knowledge within vehicle dynamics, including basic knowledge on how tires and also different differentials work. The following chapter tries to describe this so that the reader has the right basic knowledge needed.

2.1 Vehicle dynamics and models

When looking at vehicle dynamics, there are many variables of interest. Some of these includes the vehicles yaw rate, and the velocity and force generated in both lateral and longitudinal direction. Some variables can be measured directly and some of them need to be calculated or modeled. The characteristics of a vehicle is very complex and the exact behavior of a car is therefore impossible to model in every situation. There exist many different vehicle models that try to describe the characteristics of a car as adequately as possible. All the calculations for these models are to be done on a vehicles on board computer, which means that the model has to be simple enough to not reach the computer's limited computing capacity.

2.1.1 The bicycle model

The bicycle model [1] is a rather simple model that can be used to describe vehicle dynamics when turning, i.e. when we have a yaw rate and lateral forces that are affecting the vehicle. The model's major simplifications are that the mass of the vehicle is seen as one center of gravity point and that the two front wheels and the two rear wheels are combined into one wheel respectively as can be seen in Figure 2.1. These simplifications means that there is no difference in forces on the two sides, i.e. there will be no roll

effect to the outside wheel when turning in a corner. There is also an assumption made that there will be no pitch effect on the vehicle, which means that there is no suspension system that is effecting it. The model also assumes that there is no driving torque generated to the wheels, and therefore only lateral forces on the vehicle.

For most cornering situations, these assumptions work fine, and the model gives a good idea on how different parameters are affected. Despite this, one has to bear in mind that these assumptions could result in rather large errors during certain driving situations.

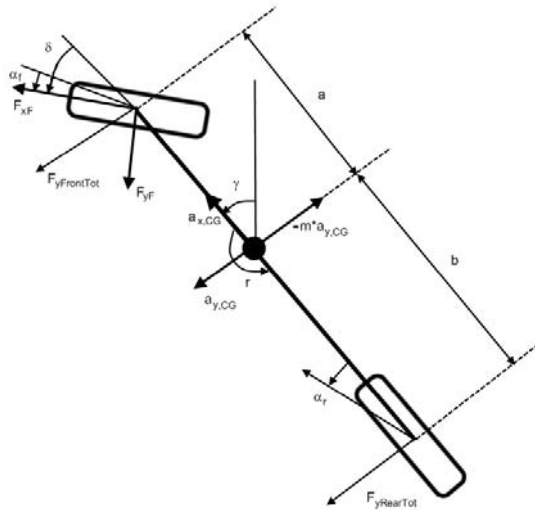


FIGURE 2.1: Bicycle Model. [2]

The total lateral force acting on the vehicle will depend on the combined forces that the front and rear tires contribute. By using Newtons second law of physics, $F_y = m \cdot a_y$, the total lateral force acting on the vehicle will be:

$$F_y = m \cdot a_y = F_{yR} + \cos(\delta) \cdot F_{yF} + \sin(\delta) \cdot F_{xF} \quad (2.1)$$

where m denotes the vehicle mass and δ is the front wheel steering angle. The acceleration in the center of gravity can be described as:

$$a_y = \dot{v}_y + \frac{F_c}{m} \quad (2.2)$$

where \dot{v}_y is the actual change of velocity in lateral direction and the centripetal force in the center of gravity, F_c , depends on the yaw rate:

$$\dot{\psi} = \frac{v_x}{R} \quad (2.3)$$

$$F_c = \frac{m \cdot v_x^2}{R} = m v_x \cdot \dot{\psi} \quad (2.4)$$

where R is the radius of the turn and v_x the velocity in the direction that the vehicle is pointing. By combining Equations 2.2 & 2.4, the acceleration can be described as:

$$a_y = \dot{v}_y + v_x \cdot \dot{\psi} \quad (2.5)$$

When combining Equations 2.5 & 2.1 the three different lateral force components that are effecting the vehicle interact as:

$$F_{yR} + \cos(\delta) \cdot F_{yF} + \sin(\delta) \cdot F_{xF} = m \cdot (\dot{v}_y + v_x \cdot \dot{\psi}) \quad (2.6)$$

If taken one step further, the lateral force components can describe the torque created around the z-axis in the center of gravity:

$$M_z = I_z \cdot \ddot{\psi} = a \cdot (\cos(\delta) \cdot F_{yF} + \sin(\delta) \cdot F_{xF}) - b \cdot F_{yR} \quad (2.7)$$

where a and b are the lever lengths from the center of gravity to the front respective the rear axle and $\ddot{\psi}$ the yaw acceleration.

When looking at the bicycle model, the assumption is that the longitudinal force is negligible. This means, as mentioned earlier, that the lateral force will almost only depend on the tire slip angle created by the front-wheel steering angle and the angle to the direction the front wheel is heading towards. When assuming this model with only two wheels, the slip angles for the front respective rear tire will be:

$$\alpha_F = -\arctan\left(\frac{v_y + \dot{\psi} \cdot a}{v_x}\right) + \delta \quad (2.8)$$

$$\alpha_R = -\arctan\left(\frac{v_y - \dot{\psi} \cdot b}{v_x}\right) \quad (2.9)$$

This angle is defined to be the angle between the direction of the tire and the direction of the velocity of the wheel. A number of interpretations can be made from these formulas. One is that the steering angle only directly influences the slip angles of the front wheels. Another is that if the numerator in Equation 2.8 goes to zero, which means that the lateral velocity plus the yaw rate is zero, the slip angle of the front wheel is equal to the front-wheel steering angle. This means that the vehicle is gliding straight forward

regardless of the steering angle. Another conclusion is that if $\dot{\psi} \cdot b$ is larger than v_y , in Equation 2.9, the numerator will become less than zero and the slip angle of the rear wheel will move to the other side on the x-axis. This happens when a vehicle takes a corner more aggressively, which means higher longitudinal velocity compared to the radius of the corner, leading to higher yaw rate as can be seen earlier in Equation 2.3.

The lateral forces acting on the front and rear wheels can also be described as:

$$F_{yF} = 2C_F\alpha_F \quad (2.10)$$

$$F_{yR} = 2C_R\alpha_R \quad (2.11)$$

where C_F and C_R are the cornering stiffness coefficients for the front and the rear tire, respectively. The above calculations are taken from [3].

A steering response, B , can be defined from these two forces [2]:

$$B = F_{yR} - F_{yF} \quad (2.12)$$

If B is 0, we have equal amount of lateral force distributed on the front and the rear wheels respectively. Theoretically, this means that with a constant steering angle, the radius of the corner will be the same for all velocities. With $B < 0$, a smaller steering angle is needed to keep the same cornering. If $B > 0$ on the other hand, the steering will have to be greater to keep the same radius of the corner. This is one way of defining the so called over- and understeer phenomena. A slight understeer is usually desired for commercially available cars because handling of the vehicle becomes easier and the risk of skidding is reduced.

2.1.2 Two track vehicle model

The bicycle model described earlier is a simplified vehicle model that only captures the main characteristics well in most situations. The fact that it is modeled by only one wheel per axis means that the forces on the two wheels on the same axis will be modeled exactly the same. In reality, there will of course exist factors that affect the two wheels differently, e.g. when cornering, the normal force will be transferred from the inner to the outer wheel. If a car uses an FXD, the active differential will in certain situations transfer torque from one shaft to the other. The effect that the FXD contributes with will be described further on in a later section of the paper. A model that is slightly more complicated than the bicycle model and tries to capture these lateral differences, is the two track model seen in Equation 2.2.

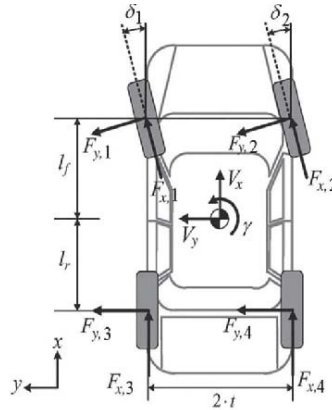


FIGURE 2.2: Forces acting on the vehicle with a two track model.

A couple of assumptions are made in this report when considering the two track model. There will never be a steering angle on the rear wheels and also the steering angle of the two front wheels are considered to be identical. Cars that are using an FXD are exclusively front wheel driven, and therefore the rear wheels will never contribute with positive forces.

2.1.3 Normal forces

The longitudinal and lateral forces generated by a tire are dependent on the normal force acting on the tire. It is therefore interesting to know how large normal force that's acting on each tire.

2.1.3.1 Lateral load transfer

Without any lateral acceleration, the normal forces on the right and left hand side of the vehicle, as seen in Figure 2.3, can be described as:

$$F_{zL} + F_{zR} = mg \quad (2.13)$$

With lateral acceleration affecting the vehicle, a torque will occur that changes the normal forces on the two sides:

$$\begin{aligned} F_{zR} &= \frac{mg}{2} + \frac{m \cdot a_y \cdot CGH}{T_w} \\ F_{zL} &= \frac{mg}{2} - \frac{m \cdot a_y \cdot CGH}{T_w} \end{aligned} \quad (2.14)$$

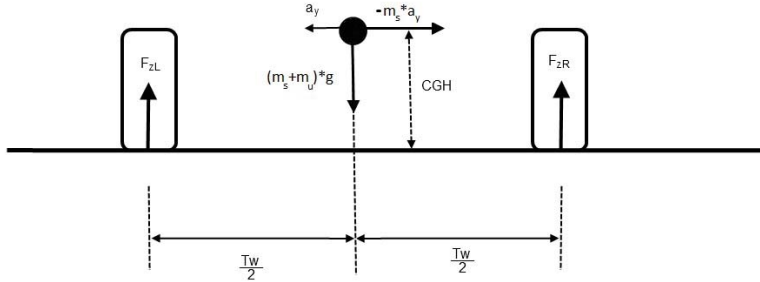


FIGURE 2.3: Normal force on the vehicle seen from the front.

where T_w is the track width (distance between the left and right wheels), a_y is the lateral acceleration and CGH is the height from the ground to the center of gravity. The torque that is an effect of the lateral acceleration in Equation 2.14, does not take into account that the center of gravity height will change during driving.

Using Equation 2.14 will result in a large stationary error because the unsprung mass isn't considered. The unsprung mass is the weight of the wheel, the wheel carrier and half the suspension weight. This mass won't be a part of the load transfer because it's fixed relative to the ground. In other words, this mass can't affect the normal force acting on the other three wheels. The corrected equations become:

$$\begin{aligned} F_{zR} &= \frac{(m_{sprung} + m_{unsprung}) \cdot g}{2} + \frac{m_{sprung} \cdot a_y \cdot CGH}{T_w} \\ F_{zL} &= \frac{(m_{sprung} + m_{unsprung}) \cdot g}{2} - \frac{m_{sprung} \cdot a_y \cdot CGH}{T_w} \end{aligned} \quad (2.15)$$

2.1.3.2 Longitudinal load transfer

The normal forces on the front and rear for a vehicle without any acceleration, as seen in Figure 2.4, is simply the gravitational force acting on the vehicle:

$$F_{zF} + F_{zR} = mg \quad (2.16)$$

Note that F_{zR} denotes the normal force of the rear and not the right hand side like in the previous section. With longitudinal acceleration, the normal forces on the front

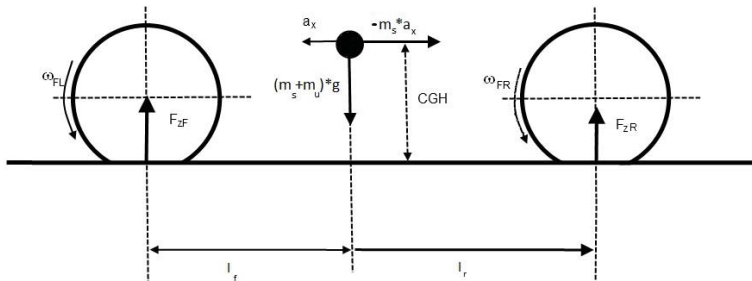


FIGURE 2.4: Normal force on the vehicle seen from the side.

respectively the rear will change:

$$\begin{aligned} F_{zF} &= mg \cdot \frac{l_f}{l_f + l_r} - \frac{m \cdot a_x \cdot CGH}{l_f + l_r} \\ F_{zR} &= mg \cdot \frac{l_r}{l_f + l_r} + \frac{m \cdot a_x \cdot CGH}{l_f + l_r} \end{aligned} \quad (2.17)$$

where l_f and l_r are the distances from the front and rear axles to the center of gravity, respectively. As can be seen in Equation 2.17, the normal force on the front axle will decrease with a positive longitudinal acceleration. This is a negative effect for Front Wheel Driven (FWD) vehicles.

The unsprung mass will affect the longitudinal load transfer in the same way as it affected the lateral load transfer. The modified equations thus become:

$$\begin{aligned} F_{zF} &= (m_{sprung} + m_{unsprung}) \cdot g \cdot \frac{l_f}{l_f + l_r} - \frac{m_{sprung} \cdot a_x \cdot CGH}{l_f + l_r} \\ F_{zR} &= (m_{sprung} + m_{unsprung}) \cdot g \cdot \frac{l_r}{l_f + l_r} + \frac{m_{sprung} \cdot a_x \cdot CGH}{l_f + l_r} \end{aligned} \quad (2.18)$$

2.1.3.3 Longitudinal and lateral load transfer combined

To be able to determine the normal forces acting on a single wheel the longitudinal and lateral load transfer need to be combined since both of them affect each wheel in some way. By calculating how many percent of the total normal force that's acting on the left side and how many percent of the total normal force that's acting on the front axle and then multiplying these factors with the amount of the total normal force acting on the

front left wheel will be given in percent.

$$\%F_{zFrontLeft} = \%F_{zFront} \cdot \%F_{zLeft} \quad (2.19)$$

$$F_{zFrontLeft} = \%F_{zFrontLeft} \cdot (m_{sprung} + m_{unsprung}) \cdot g \quad (2.20)$$

The same analogy is true for the other three wheels.

2.2 Tire dynamics

A gas-inflated tire that is non loaded will have a radius called unloaded radius. When a tire is loaded, and therefore have a normal force acting on it from the road, it will deform against the road creating a contact area. The contact area is proportional to the load, where more load gives a larger contact area. The deformation of the tire will lead to a shorter distance between the center of the tire and the road, this is denoted the loaded radius.

A loaded tire's contact area against the road can be divided into two parts; adhesion area and sliding area (Figure 2.5). The adhesion area is the part of the contact area that's said to adhere to the road, which means that this part hasn't reached the friction limit yet, but it can still handle more force without sliding. The sliding area is the area that has reached the friction limit and thus has begun sliding. How this area is divided depends on a number of factors but it can basically be divided into two cases, longitudinal forces and lateral forces which will be explained further on.

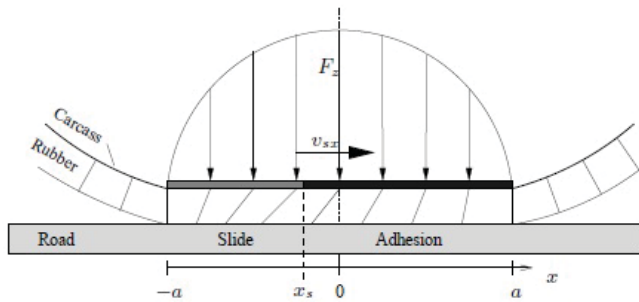


FIGURE 2.5: Adhesion area and sliding area of a tire. [4]

2.2.1 Longitudinal forces

Rotating the tire will result in compression of the tire where it hits the road and expansion where it leaves the road. The tire itself has a dampening effect meaning that all energy used to compress the tire won't be recovered when it expands again. This loss in force is called rolling resistance, F_{rr} . F_{rr} is often modeled as being proportional to F_z with the proportionality constant f (Equation 2.21). A typical value of f is 0.015 for passenger cars [3]. The compression and expansion of the tire will also move the normal force acting on the tire in front of the center line (Figure 2.6) when the tire is rolling. The moved normal force will result in a third radius of the tire, the effective rolling radius. This is the radius related to the actual linear longitudinal velocity of the rolling tire and it is longer than the loaded radius but shorter than the unloaded radius.

$$F_{rr} = fF_z \quad (2.21)$$

Applying torque on the tire will generate longitudinal force moving the tire forwards or

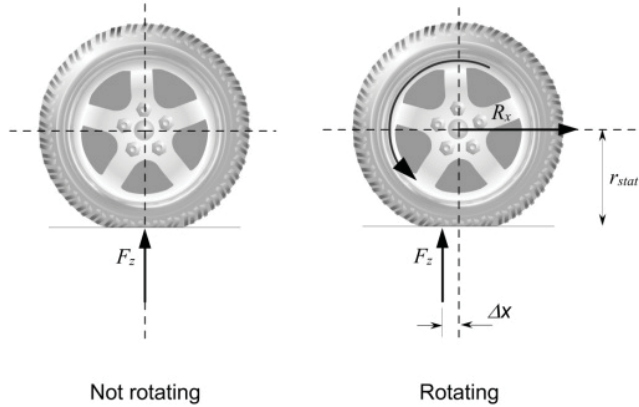


FIGURE 2.6: Normal force acting on the tire. [3]

backwards. Doing so will always generate a longitudinal slip, called slip ratio. This is a ratio of the difference between the angular velocity of the tire and the angular velocity of the corresponding undriven wheel. The slip ratio is defined as:

$$\kappa = \frac{R_e\omega - V_x}{V_x} \quad (2.22)$$

where V_x is the undriven wheel speed and $R_e\omega$ is the angular velocity of the driving wheel. This leads to the following slip ratio relationships:

$$\text{Locked} : \omega = 0 \Rightarrow \kappa = -1 \quad (2.23)$$

$$\text{Free rolling} : \omega = \frac{V}{R_e} \Rightarrow \kappa = 0 \quad (2.24)$$

$$\text{Spinning} : \omega = 2\frac{V}{R_e} \Rightarrow \kappa = 1 \quad (2.25)$$

The amount of slip will be one of the factors that decide the ratio between adhesion area and slip area for the tire's contact area. The more slip the bigger slip area. The slip area will grow with the slip from the backside of the contact area. When the sliding area is as big as the contact full tire spin occurs. When braking the sliding area will grow from the front and be as big as the contact area when the tire is completely locked. With the same analogy the adhesion area will be as big as the contact area when the tire is free rolling.

The maximum longitudinal force that can be generated is proportional to the normal force with the friction coefficient, μ , as proportionality constant:

$$F_{x,max} = \mu F_z \quad (2.26)$$

The generated longitudinal force depends on the longitudinal slip ratio. In Figure 2.7 the force slip ratio curves for different road conditions can be seen. The longitudinal force is normalized against the normal force and hence it's the friction coefficient shown on the y-axis. By looking at the graph the characteristics of a tires longitudinal force generation can be seen. For low slip ratios the force curve is linear, at a specific slip ratio a maximum is reached and after that it slowly decays. Different road conditions have different coefficients of friction which is reflected by the maximum values for the different curves.

2.2.2 Lateral forces

Lateral forces will be generated when the vehicle is turning, or more specifically when there is a difference in the angles of the front tires relative to the angle of the vehicle. When turned, the tire won't travel in the direction of its orientation and there will be a slip between the tires orientation and the velocity vector. This lateral slip is called slip angle since it can be expressed as an angle.

As can be seen in Figure 2.8 the lateral force is proportional to the slip angle for small slip angles. For larger slip angles the lateral force converges. In difference to the longitudinal

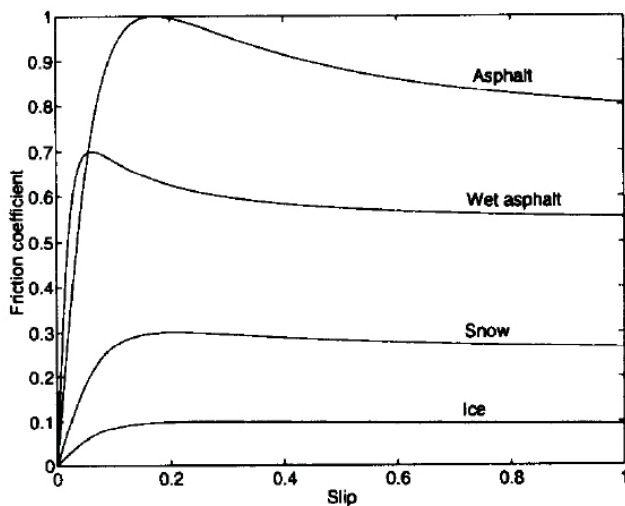


FIGURE 2.7: Friction coefficient as a function of slip ratio for a tire. [5]

force the lateral force won't decrease for very large slip angles. This doesn't mean that max steering wheel angle always generates maximum lateral force. In many situations a too large steering wheel angle will over turn the wheel and start decreasing the slip angle hence generating less lateral force.

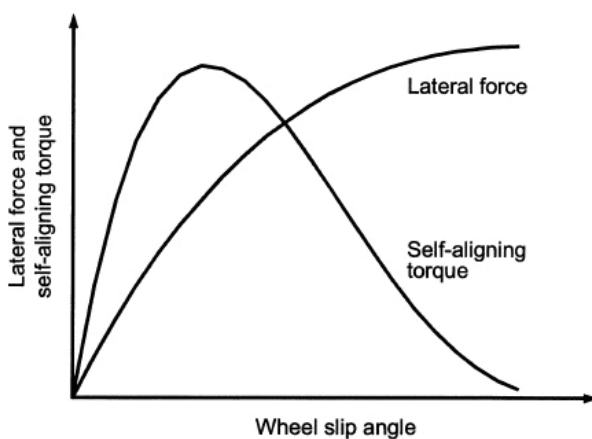


FIGURE 2.8: Lateral force as a function of slip angle for a tire. The self aligning torque can also be seen. [6]

The slip angle is another factor that will decide the ratio between adhesion area and sliding area. When the slip angle is large enough the whole contact area will be in the sliding region, hence the maximum lateral force is generated.

In Figure 2.8 the self-aligning torque can also be seen. This is a force generated due to the uneven force distribution over the tires contact area when it's turned. This force increases fast for small slip angles and is the counter force felt in the steering wheel when turning. At a certain point it drops again and this is the locking feeling that's felt in the steering wheel when turning sharp enough.

2.2.3 Combined slip

Since the longitudinal and lateral forces depends on slip ratio and slip angle it's necessary to combine these slips to be able to combine the forces. The total force in any direction can never exceed the normal force times the friction coefficient:

$$F_{total} \leq \mu F_z \quad (2.27)$$

The total force can be expressed as:

$$F_{total} = \sqrt{F_x^2 + F_y^2} \quad (2.28)$$

Figure 2.9 describes these relations well. It has also been mentioned that both slip ratio

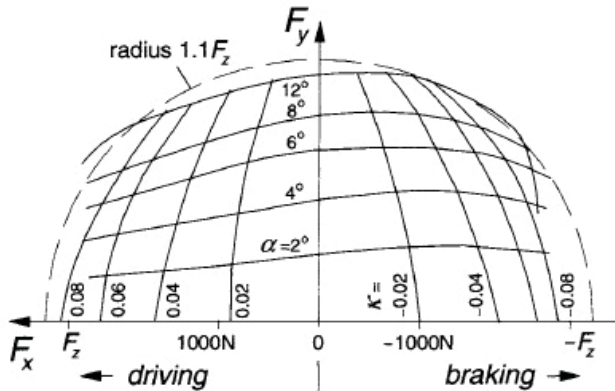


FIGURE 2.9: Longitudinal force and slip ratio on the x-axis and lateral force and slip angle on the y-axis. These forces combined can not exceed the circle (Equation 2.28) that is the total force expressed as Equation 2.27. [7]

and slip angle affects the ratio between adhesion area and sliding area. In analogy with Figure 2.9 the sliding areas generated by slip ratio and slip angle will be combined.

2.2.4 Tire stiffness

There are many parameters that need to be known about the vehicle in order to estimate the friction well. One parameter that is not known (unless specified) is the stiffness of the tires. A tire has two specified stiffnesses, longitudinal and lateral stiffness. The longitudinal stiffness describes how much a tire will deform while being loaded longitudinally, for example when accelerating or braking. The vertical stiffness describes how the tire deforms while being loaded vertically, for example when turning.

The tire stiffness is a very important parameter to describe how much force a tire can generate. The force generated from the ground through the tires can, in the linear region, be described as a function of the tire stiffness and the slip ratio. Hence, force generated per slip ratio is proportional to the tire stiffness. Longitudinal and lateral force as functions of stiffness and slip ratio in the linear region are described by:

$$F_x = C_x \cdot \kappa \quad (2.29)$$

$$F_y = C_\alpha \cdot \alpha \quad (2.30)$$

Once again it should be stressed that this is only valid in the linear region of the force per slip ratio curves. Thus, the theoretical definition of the tire stiffness is the gradient of the force per slip ratio around the origin.

Different tires can have very different tire stiffness, which of course will have a great impact on the tires performance. Winter tires are less stiff due to a softer rubber compound. Generally, this also means that snow tires reach their maximum generated force at a larger slip ratio than summer tires. In the same way an extra stiff racing tire will reach its maximum force at a smaller slip ratio. The tire stiffness should not have to be set beforehand (meaning that the driver would have to specify if he/she changes tires) and therefore need to be estimated for an accurate friction estimation.

2.3 Tire models

There are several models to describe a tire mathematically. These models can be divided into four categories, empirical models, semi-empirical models, simple physical models and complex physical models.

Empirical models describe tire characteristics that are acquired from measurements of the tire. To fit the curve according to measured data the parameters are assessed with methods like regression. A well-known empirical model is the Magic Formula [7]. This model provides good fit for F_x , F_y and M_z curves and have coefficients which are easy to interpret.

Semi-empirical models can use a similarity method, which means that some calculations are replaced by known or measured data. By distorting, rescaling and multiplying the result, new relationships are acquired which can describe the tire in different situations. For example one can observe that the pure slip ratio curves shape doesn't change much [7] when the tire runs on different conditions. By shifting the nominal curve these conditions can be described.

The physical models are purely analytical and aims to describe the tire with the help of its physical characteristics. A simple physical model uses simple mechanical representation and can be calculated fairly easy by hand. This often results in pretty poor accuracy but sometimes that's enough. To get better accuracy a more complex model can be set up and simulated in a computer using aids like the finite element method.

In Figure 2.10 some modeling characteristics and how they behave depending on category can be seen.

2.3.1 Brush model

The brush model is a highly used simple physical model. The idea is to model the tire surface as a row of elastic bristles which deflect in different directions depending on how the tire is loaded. This model is illustrated to the left in Figure 2.11.

For pure side slip ratio the bristles will deflect in the direction of the y-axis, which can be seen at the top right in Figure 2.11. In the same figure pure brake slip ratio can be seen, that is when the bristles deflect in the direction of the x-axis. Finally at the bottom right of this figure combined slip is illustrated.

In Figure 2.12 it can be seen how different slip angles affect the tire. Small slip angles gives a large adhesion area (flat part) and a small sliding area (curved part). As the slip angle increases a larger number of bristles reach their maximum deflection, hence increasing the sliding area. At a certain slip angle all bristles have reached their maximum deflection and this results in full sliding.

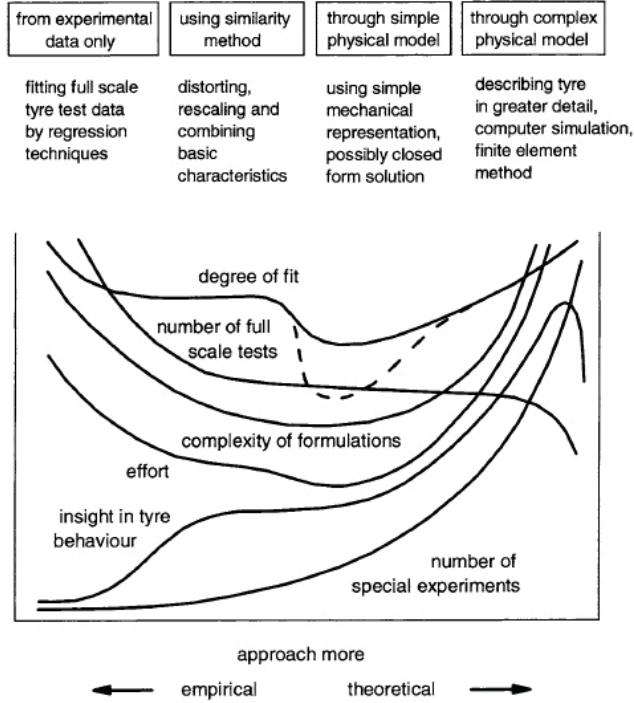


FIGURE 2.10: Four categories of possible types of approach to develop a tire model. [7]

The longitudinal force described by the Brush model [7]:

$$F_x = \frac{C_x \left(\frac{\kappa}{1+\kappa} \right)}{f} F \quad (2.31)$$

where:

$$F = \begin{cases} f - \frac{1}{3\mu F_z} f^2 + \frac{1}{27\mu^2 F_z^2} f^3, & \text{if } f \leq 3\mu F_z \\ \mu F_z, & \text{otherwise} \end{cases} \quad (2.32)$$

and:

$$f = C_x \frac{\kappa}{1 + \kappa} \quad (2.33)$$

2.3.2 The Magic Formula tire model

The Magic formula is a series of tire design models developed by H. Pacejka [7] in collaboration with Volvo. The formula is a well known empirical model which has been

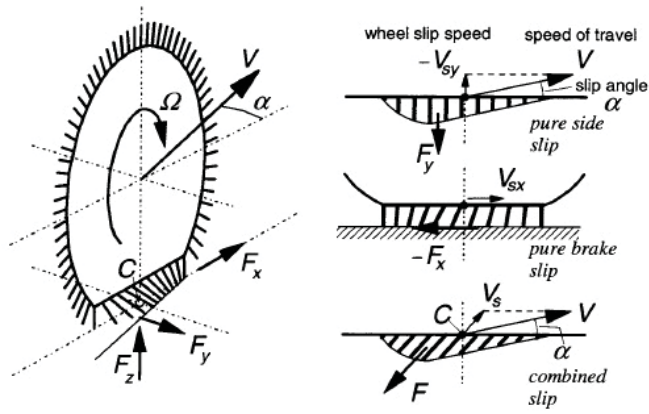


FIGURE 2.11: The brush tire model. [7]

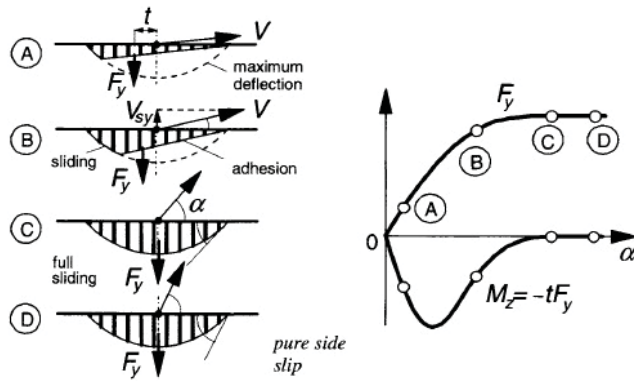


FIGURE 2.12: The brush tire model. [7]

given its name due to no physical basis for the structure of the equation. It models the fact that different tires have various characteristics which influence the final force generated from the contact patch to the ground. The formula is very complex, where numerous parameters for each tire can be used to calculate lateral and longitudinal forces and also self-aligning torque depending on the slip angle or slip ratio. In this report, the Magic formula is kept fairly simple to show the idea behind the model, rather than getting a profound understanding behind the development of the model.

The formula is defined as:

$$y = D \sin[C \arctan Bx - E(Bx - \arctan Bx)] \quad (2.34)$$

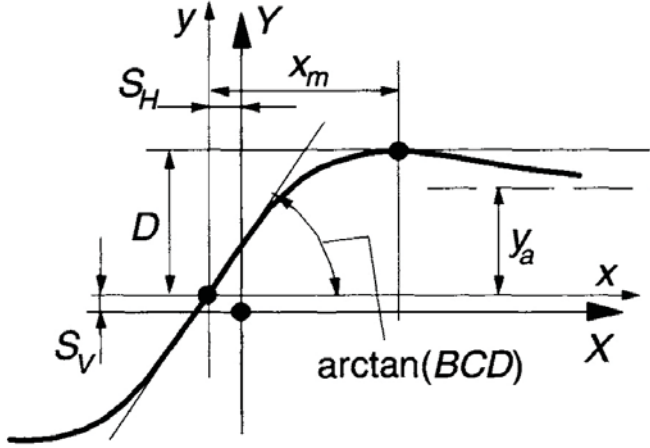


FIGURE 2.13: The Magic formula parameters and its influence. [7]

where the four fixed constants are:

- B is the stiffness factor.
- C is the shape factor.
- D is the peak factor.
- E is the curvature factor.

y is the output, either lateral or longitudinal force, dependent on x which is either slip angle, α , or slip ratio, κ . The input and output can be affected by an offset, S_V and S_H , so the curve doesn't pass through the origin.

$$Y(X) = y(x) + S_V \quad (2.35)$$

$$x = X + S_H \quad (2.36)$$

The stiffness factor, B , depends on the cornering stiffness, $C_{F\alpha}$:

$$B = \frac{C_{F\alpha}}{CD} \quad (2.37)$$

$$C_{F\alpha} = c_1 \sin(2 \arctan(\frac{F_z}{c_2})) \quad (2.38)$$

where c_1 and c_2 is the maximum cornering stiffness and the load at maximum cornering stiffness, respectively.

D is the maximum lateral or longitudinal force:

$$D = \mu \bar{F}_z \quad (2.39)$$

The shape and curvature factors can be described as:

$$C = 1 \pm \left(1 - \frac{2}{\pi} \arcsin \frac{y_a}{D}\right) \quad (2.40)$$

$$E = \frac{Bx_m - \tan \frac{\pi}{2C}}{Bx_m - \arctan(Bx_m)} \quad (2.41)$$

where x_m is the distance on x-axis from x_0 to the peak of the curve and y_a is the distance on the y-axis from y_0 to the level where the curve converges.

All of these parameters and how they influence the curve can be seen in Figure 2.13.

2.3.3 Dugoff tire model

The longitudinal force described by the Dugoff tire model [8] is defined as:

$$F_x = f_i \cdot \frac{C_x \cdot \kappa}{1 - \kappa} \quad (2.42)$$

where:

$$f_i = \begin{cases} \lambda \cdot (2 - \lambda), & \text{if } \lambda < 1 \\ 1, & \text{otherwise} \end{cases} \quad (2.43)$$

and:

$$\lambda = \mu \cdot F_z \cdot \frac{(1 - \kappa)}{2 \cdot C_x \cdot \kappa} \quad (2.44)$$

The model depends on four parameters; the slip ratio, the longitudinal tire stiffness, the normal force and the tire/road friction coefficient. Assuming that the slip ratio is the only dynamic parameter during driving, means that λ will be smaller than 1 when the slip ratio is small enough. When $f_i = 1$ the force will only depend on the longitudinal tire stiffness and the slip ratio, meaning that the friction coefficient and normal force has no impact.

2.3.4 The BW tire model

This tire model is developed by Ola Nockhammar at BorgWarner TorqTransfer Systems AB in Landskrona. It's more complex than the Brush and Dugoff model but still simple to use. Instead of just having the tire stiffness as a parameter to alter the behavior of

a tire, a second parameter, ξ , is introduced. ξ will alter the inclination of the force per slip ratio curve. This results in a tire model with two degrees of freedom instead of just one like the Brush and Dugoff models. A higher degree of freedom makes it easier to adjust the model for different kinds of tires which is a great advantage.

Due to confidential reasons this model can't be explained in any greater detail.

2.4 Differentials

When driving along a straight line on a road with equal friction for all wheels, both driven wheels will have equal torque and velocity. In this situation a differential wouldn't even be necessary. The differential is needed when the vehicle is cornering. In this situation the different wheels will have different turning radii, thus requiring different angular velocities. This is the general idea behind a differential, to be able to have different angular velocities of the driven wheels. Without a differential it would be very hard to turn the vehicle, especially at low velocities, since equal speed of the wheels prevents the rotating movement happening while turning.

2.4.1 Open differential

The open differential is the classic differential used in most cars today. With an open differential, the torque will always be evenly distributed to the two driving wheels. One wheel can not have higher torque than the other wheel but they can have different angular velocities. This behavior is directly related to the mechanical construction of the open differential which can be seen in Figure 2.14.

The angular velocities of the two side gears and the crown wheel can be described as:

$$\omega_r = \frac{\omega_1 + \omega_2}{2} \quad (2.45)$$

2.4.2 Problems with the open differential

A situation that creates a problem for a vehicle with an open differential, is when one driven wheel has significant lower friction to the ground than the other. The wheel with low friction can only handle relatively low torque before it starts spinning. This means that the torque applied to the two drive shafts will be restricted by the wheel with the lowest friction to the ground due to the torque splitting nature of the open differential.

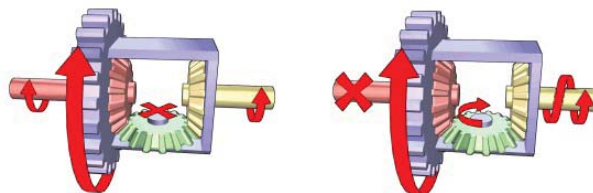


FIGURE 2.14: The open differential. To the left is the case of equal wheel speeds, to the right is one wheel completely stationary while the other wheel still rotates. [9]

This will in turn reduce the traction of the vehicle. Two possible scenarios for when the friction force to the ground might differ between the driven wheels are when the road is partly covered in ice and when cornering at high velocities which will make the inner wheel lift from the ground.

When driving on a split- μ (different friction coefficients for the driven wheels) surface, the wheel on the low friction area will easily reach maximum force before it starts to spin. The force it can transfer to the ground will thus be the restricted which in turn will restrict the torque applied on the other wheel. The result of all this is that even though only one wheel has bad grip to the ground the traction is still greatly reduced.

The other scenario, when cornering at a high velocity leading to the inner wheel lifting, will give the same effect. The normal force acting on the inner wheel will be reduced when it lifts. This will reduce the force that can be transferred to the ground which will reduce the amount of torque that can be applied to the drive shafts. In a worst-case scenario the inner wheel has lost contact to the ground completely reducing the transferred force to the ground to zero. The only torque applied is to spin the wheel and this is almost no torque at all compared to the torque used to propel the vehicle. The propulsive power will be zero and the vehicle will lose velocity. After a while the inner wheel will touch the ground again and some force will be transferred only to lift the wheel up again. This will get the vehicle stuck oscillating around this inefficient boundary wasting lots of power.

A solution for these two different scenarios would be to lock the two drive shafts together. This would keep torque applied to the outer wheel even when the inner wheel loses grip, but the fundamental idea of the differential would be lost. That is, the possibility of a speed difference between the two drive shafts. This would also affect the steering behavior in several bad ways, especially at lower velocities. Hence it would be very beneficial to be able to lock the drive shafts together in certain situations. It would be even more beneficial if they were coupled with a device where some slip were allowed

between the shafts, making it possible to control the amount of torque transferred from one shaft to the other.

2.4.3 Limited slip differential

The idea of a Limited Slip Differential (LSD) is not to apply more torque to a wheel than it can transfer to the ground. This means that the torque splitting nature of an open differential needs to be countered. Take the sharp turn example from above. The lateral forces of the vehicle will lift the inner wheel from the ground which will result in less traction. With an LSD the torque distribution can be managed so that more torque is applied on the outer wheel. The vehicle will gain more traction when cornering with an LSD than with an open differential. The same effect is applied when driving on a split- μ surface. Torque is transferred from the wheel with lower friction to the ground to the wheel with higher friction to the ground to increase the traction.

There are different types of LSDs, they can be divided in two main categories, passive and active LSDs. Passive LSDs are designed in such a way that they do the torque distribution without any required activity from the outside. The Torsen differential is a brilliant example of a passive differential. A complex set of worm gears and spur gears results in a differential that does the torque distribution by itself when needed. Passive differentials require little effort to use but the properties of the differential can't be changed in any way. Active differentials are controlled from the outside. The amount of torque transferred from one shaft to the other can be freely controlled and this gives much more power over the vehicles behavior.

2.4.4 FXD

The FXD is an electronic Limited Slip Differential made by BorgWarner AB for FWD cars. It uses the same clutch technology as their four wheel drive systems. Instead of using the clutch to transfer torque between front and rear it's used to transfer torque between the left and right front wheels. The fact that the clutch is actuated from the outside is what makes the FXD an active limited slip differential where the torque transferred between the wheels is freely controlled.

2.4.4.1 The clutch

The clutch is based on BorgWarner's Gen5 electro-hydraulic clutch. It's engaged by building a hydraulic pressure forcing the clutch plates together resulting in a torque

transfer. The pressure is built up by a hydraulic pump operated by an electric DC motor. The quick and exact control nature of the DC motor results in the clutch being very accurate. The amount of torque transferred through the clutch is easily managed with a rather simple electric signal and above all changed can be made very quickly. This is positive when used in cars because things happen very fast.

2.4.4.2 The differential

The differential is basically an open differential but with one major difference, the electro-hydraulic clutch. The clutch is installed in a way that makes it possible to couple one of the drive shafts together with the differential housing. This gives the possibility to transfer torque from one shaft to the other in certain situations. One of these situations is when one wheel has less grip than the other wheel and torque can then be transferred to the wheel with the most grip. When cornering hard or driving on a split- μ surface the clutch will be engaged allowing for the torque distribution to be altered.

2.4.4.3 Control algorithm

It's been stated that the FXD itself is very easy to control but to get any real function from it, it needs to be controlled in a smart way. The algorithm controlling the FXD is complex and powerful. It uses several measured signals from the vehicle which it receives via the CAN bus to calculate the best possible amount of torque to transfer at any time while driving.

2.4.4.4 Benefits of the FXD

The most obvious benefit of being able to distribute torque freely between the driven wheels is used in several ways to create even more benefits. The overall traction of the vehicle when cornering or running on split- μ surface is improved to begin with. Since it's an active LSD it's much easier to avoid heavy under steer compared to passive LSDs where the locking torque can't be controlled at any given moment. It's a lightweight alternative compared to All Wheel Drive (AWD) to improve traction performance and it can prevent torque steer.

A major safety benefit is the yaw damping feature. Being able to lock the driven wheels together in an avoidance maneuver will make the vehicle less likely to spin out of control since the locked wheels will prevent the vehicle from rotating around its own axle. Another benefit to safety is the fact that it's an active LSD. This means that

torque transfer can cease immediately in favor of the Anti-lock Breaking System (ABS) and ESP systems when needed. When this need to happen really fast the DC motor operating the hydraulic pump is short circuited which will make it stop instantaneously releasing all pressure on the clutch.

Chapter 3

Friction

This chapter will describe friction in a more detailed manner; what it is and how it affects a vehicle.

3.1 What is friction?

Friction is the force that resists one element of material sliding against another. There are several types of friction, one of them is dry friction which resists relative lateral motion of two solid surfaces in contact. Hence dry friction is the force that one must overcome to pull a box along a floor. Dry friction is the friction that's important for this work. Further on, dry friction can be divided in two, static friction and kinetic friction. Coulomb friction is a model used to approximate dry friction. It's expressed as:

$$F_f \leq \mu F_n \tag{3.1}$$

where:

- F_f is the frictional force which is parallel to the surface and has a direction opposed the applied net force.
- μ is the coefficient of friction, different for different surfaces.
- F_n is the normal force exerted by each surface on the other.

This model provides a threshold for how much side force that can be applied before an object starts to move laterally. As long as the side force is less than or equal to the normal force multiplied by the coefficient of friction an equal amount of friction force

will be generated in the opposite direction, thus preventing the object from moving. How much force that is needed to move an object along a surface is thus decided by two factors; the normal force acting on the object and the coefficient of friction between the two surfaces. When the applied side force gets larger than this threshold the object will start to move, hence leaving the static friction region and entering the kinetic friction region. The maximum side force that can be applied before an object starts moving is known as traction which is a common term when dealing with vehicles. It's simply how much longitudinal/lateral force a tire can handle before it loses the grip to the road and starts sliding.

The coefficient of friction for static friction is denoted as μ_s and the one for kinetic friction as μ_k . Generally the kinetic coefficient of friction is lower than the static one. This means that the side force needed to make an object move is larger than the force needed to keep it sliding. The friction coefficient between two materials needs to be determined empirically and it cannot be calculated.

3.2 Tire/road friction

Tire/road friction is, as the name suggests, the friction between tire and road. Normally the tire road friction coefficient is within the range 0.1 - 1, 0.1 for bad tires on ice and 1 for good tires on dry asphalt. Rewriting Equation 3.1 gives:

$$\frac{F_f}{F_n} \leq \mu \quad (3.2)$$

Having it on this form makes it easier to understand what a certain coefficient of friction really means for the vehicle. Having a coefficient of friction equal to 1 means that the force of friction can be as large as the normal force acting on the tire. This also means that the force of friction for all tires can be as large as the normal force acting on the whole vehicle. Let's have an example. A vehicle has a mass of 1 300 kg. Let's assume that it's driving at a completely horizontal asphalt road with a coefficient of friction equal to 1. Since the road is horizontal the normal force acting on the vehicle can be expressed as:

$$F_n = mg \rightarrow F_n = 12766N \quad (3.3)$$

Having a coefficient of friction equal to 1 means that the force friction can be equal to the normal force without the vehicle losing grip. Thus, 12766 N of force can be used to accelerate the vehicle or 12766 N of force can be generated while cornering or braking without the vehicle losing grip. Cornering and accelerating can be done at the same

time, as long as the total amount of force the tires need to handle won't rise above 12766 N .

The example above is extremely simplified and there are lots of other factors coming into play when a vehicle is accelerating or cornering but it still gives a good idea about the properties of tire/road friction. A coefficient of friction equal to 1 means that a force of friction equal to 100 % of the normal force can be generated and a coefficient of friction equal to 0.1 means that a force of friction equal to 10 % of the normal force can be generated.

The example also illustrates another important point. A vehicle can never accelerate faster or corner harder than 1 G (9.82 m/s^2), unless some kind of downforce is generated.

3.3 Downforce

Downforce is a downward force generated by the aerodynamics of a vehicle. The idea is to increase the normal force acting on the vehicle and by doing that more force of friction can be generated resulting in better grip. It's important to understand that the increased force of friction isn't due to a higher coefficient of friction, it's still the same. The increased grip comes purely from an increased normal force.

Chapter 4

Friction estimation method

This chapter will describe the chosen method that has been used to estimate the tire/road friction. Different approaches are weighted where a great deal of effort has been put on dealing with the fact that the method should work well in a practical manner, rather than only during simulations.

4.1 Approach

The main idea for how to estimate friction is the following. Two models describing the vehicle forces and the tire forces are used. First, all signals for the vehicle model and all signals for the tire model except the tire/road friction coefficient are derived. Next, the tire model is fitted to the vehicle model with recursive least square fitting, using the tire/road friction coefficient as fitting parameter, which will give an estimate of the tire/road friction coefficient. Finally, the estimated tire/road friction coefficient is fed back to the tire model to update the system. A flow chart of this method can be seen in Figure 4.1 This method with the two different models work because the forces generated by the tires should be equal to the total force acting on the vehicle.

One of the first parts of method includes calculations of the forces acting on the vehicle by using a vehicle model. This is for example done by using measured signals and calculated parameters such as wheel speed, yaw rate and acceleration but it can be done in other ways as well. Two different models that describe the vehicle force will be presented in this work.

Another part is to calculate the forces generated by the tires through a tire model. Such a model often depends on the tire stiffness, the tires slip ratio, the normal force acting on the tire and the road friction coefficient. Several tire models exist today and in this

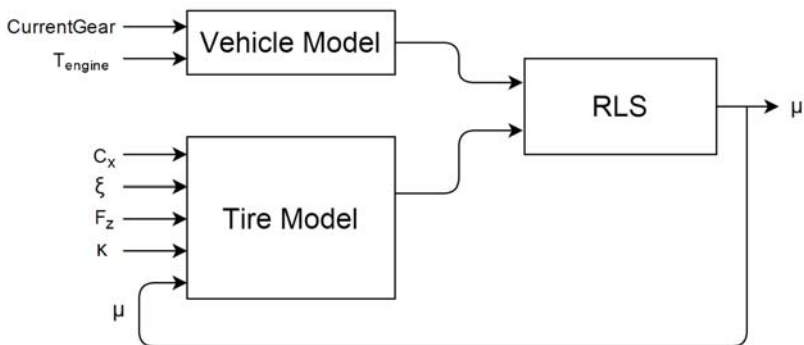


FIGURE 4.1: Simplified flow chart of the friction estimator.

work four of them are considered. One of them is ruled out almost immediately, two of them are ruled out after some more examination and the fourth is the one that is used. More on this later on.

Recursive least square (RLS) fitting is a well known fitting method with fast convergence and good features such as forgetting factor. This method will be explained in detail as well.

4.1.1 Practical restrictions and problems

The idea presented above might sound like a very simple solution but there are several problems that have to be considered. The most important aspect that has to be taken into account is the fact that the friction estimation model has to work in a real vehicle handled in actual driving situations. In a theoretical world, where a vehicle and a tire model is fed unbiased data, the friction coefficient can be obtained with good certainty and quite fast. Unfortunately, in the practical world, the data fed to the models are far from optimal. Things like measurement noise and approximative calculations corrupt the results. Several more complex driving situations are also hard to model correctly. This can for example be excessive wheel spin, aggressive cornering or velocities close to zero.

The true dynamics of both a vehicle and a tire is very complex and therefore also difficult to describe accurately with a model. At the same time, a model that is to be used has to be simple enough so that calculations are possible on an micro controller unit with limited computational power. Even though many simplified models are shown to be accurate enough to reflect reality in most driving situations, there are times when a simplified model inaccurately describes the detailed dynamics of a vehicle or a tire.

There are also numerous models that use signals/parameters which are hard to measure or approximate well in reality. Some of these signals include the lateral velocity and slip angle. It is therefore desired to have a model that doesn't rely on these signals. There are also vehicle specific parameters, some which change between driving sequences, that can have a large impact on the modeled results. A few of these parameters include the mass of the vehicle, wheel radii, lengths from center of gravity to the rear and front axle and the center of gravity height. The same goes for tires. When changing from winter tires to summer tires the tire stiffness will change a lot which will have a large impact on the results from the tire models. When using simulations, the exact value of these parameters can be known, but in a real environment they either have to be static, approximated or neglected in computations.

4.1.2 FXD

The problem stated in this work is to estimate the tire/road friction for a vehicle using an FXD. This results in a number of conditions that have to be thought of and applied throughout the research. First of all, vehicles with an FXD installed are solely front wheel driven, meaning that there are no positive longitudinal forces acting on the rear wheels. The velocity of the rear wheels can therefore in most cases be used as a good approximation of the vehicle's reference velocity. Through the same reasoning, the longitudinal acceleration of the vehicle can be derived from the derivative of the rear wheel velocities. There is also no steering done by the rear wheels.

Another aspect that has to be considered is that the FXD is an electronic limited slip differential, which means that the torque applied to the two driving shafts can differ in certain situations, unlike for a vehicle equipped with a standard open differential.

4.1.3 Related work

There have been quite extensive amount of research within this field of study and many different model proposals related to friction estimation during the last decades. The outcome of this research usually show promising results, where the proposed solution works well during simulations and/or testing. Related work has provided a lot of information and help to this work, especially when it comes to getting a general understanding of the problem and its difficulties. But due to the fact that many results are based on theory and simulations, a lot of information could be of little use or in some cases even be misleading.

Some different approaches have been used before. Sometimes a tire model is looked upon alone to derive information about the friction. Sometimes the tire model is compared to another tire force model to fit the friction coefficient by comparing the fault between the models.

In [5] Gustafsson uses the first of the above mentioned approaches. The method is called the slip slope method and the idea is that the force per slip ratio curve for a tire will have different inclination (slip slope) depending on the friction to the road. It's also said that the distribution of the data points says something about the road condition. The data points are more widely spread when driving on snow or gravel for instance.

In [10] the authors use two models, one tire model and one vehicle model. The idea is that the tire model should match the vehicle model since ideally the forces acting on the vehicle should come from the tires. A Kalman filter is used to calculate the tire and vehicle forces. The friction coefficient is then estimated with a recursive least squares algorithm. This article uses several signals that are neither available on the CAN bus or can be calculated in any good way which makes it impossible to use.

Finally, in [8] the authors mix the methods mentioned above. A Kalman filter is used to estimate the tire forces and then the slip slope is estimated with RLS. The slip slope is then used to estimate the friction coefficient.

All these articles have flaws. Gustafsson's method is too simple and therefore not accurate enough. The other two both used unavailable signals and are unnecessarily complicated.

4.1.4 Conclusion

All in all, it is a great challenge to estimate the tire/road friction coefficient. The approach, all of the problems mentioned and how they were taken care of will be explained in greater detail later on in the report.

4.2 Signal processing

Apart from the fact that a vehicle is hard to model properly, there is an uncertainty from the signals taken from the vehicle's CAN bus. The true signal values can be distorted from measuring and process noise as well as being delayed due to calculations and approximations. Different signals can have varying distortions, and therefore include various challenges.

4.2.1 Filters

The signals that are taken from the vehicle's CAN bus usually include quite a lot of noise and can cause severe succeeding errors during calculations and approximations. This measure and process noise mainly consist of sudden unwanted changes of the signal that generally has higher frequency than the true signal value. To exclude these high frequencies, the signal is run through a low pass filter which will attenuate the amplitude of the higher frequencies. The amount of attenuation for certain frequencies depend on the filter's cutoff frequency.

In Figure 4.2, the filtered and unfiltered values can be seen for two signals, one of the wheel speeds and the other one of the engine torque. It can be seen that the noise of the signals are reduced after filtering, but to a cost of a delaying the signal. The sudden drop of the engine torque, at around 11 seconds, appear due to a gear change. This sudden drop of engine torque will be seen as a high frequency and is therefore incorrectly suppressed by the low pass filter.

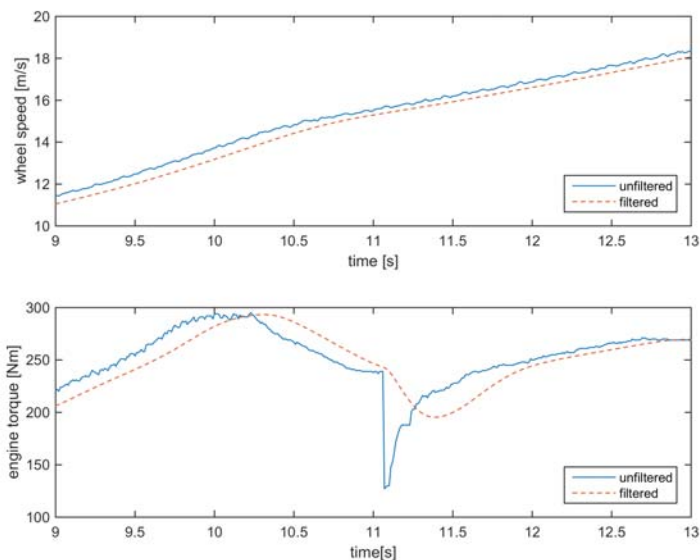


FIGURE 4.2: The unfiltered and filtered values for wheel speed, subplot one, and engine torque, subplot two. The figure shows how two different signals respond to filtering.

The amplitude and frequency of the noise will differ for various signals and could therefore be filtered with different cutoff frequencies to get the most correct value for each

individual signal. For example, the engine torque signal, seen in Figure 4.2, subplot 2, could be filtered with a higher cutoff frequency than the wheel speed, seen in Figure 4.2, subplot one, to capture its faster changing characteristic better. However, an important aspect to consider during filtering, is the duration of the delay that will affect the signal. Signals that are run through filters with different cutoff frequencies, will also have differing delay durations. In the extent, this could lead to computations that should equal one another will differ greatly due to their different signal dependencies. All signals will therefore be filtered with the same low pass filter.

In Figure 4.3, two different force models, that should be equal to each other, are dependent on different parameter and signal values. In subplot one, a signal that affect the tire model is filtered with a cutoff frequency significantly lower than the cutoff frequency for the signals affecting the vehicle model. In the extent, the force calculated from the tire model becomes delayed compared to the computed vehicle force. In subplot 2, the signals are filtered with the same cutoff frequency, hence resulting in a better match between the two models. The conclusion from this is that the low pass filters should not only be designed to get the best possible accuracy for that specific signals, but the succeeding effects also need to be considered.

4.2.2 Static parameter impact

Even if a model can recreate a driving sequence correctly, there will always be an uncertainty due to vehicle specific parameters that are used. Some of these parameters include the position of the Center of Gravity (CoG), the radius of the wheels and the mass of the vehicle. The position of the CoG will affect the lengths from the CoG to the two axles, denoted l_f and l_r respectively, and also the CoG height from the ground. The position of the CoG will change depending on how the vehicle is loaded. The radii of the wheels can change slightly over time as the tire pressures changes, and can also be different from each tire. The radius of the wheel is used to calculate the velocity of the wheel and also to convert axle torque to force generated at the edge. The mass of the vehicle can change between different driving sequences, depending on how many persons that are seated within the vehicle and also on additional weight. The vehicles mass and CoG height is used to calculate the weigh distribution and therefore also the amount of downward force generated at each tire.

To get an understanding of how much these parameters affect the result, the force generated from two models with differing parameter values are seen in Figure 4.4. In the first subplot, the longitudinal force is calculated from a vehicle model that approximates the torque applied to the two driving shafts and thereafter the force generated to the

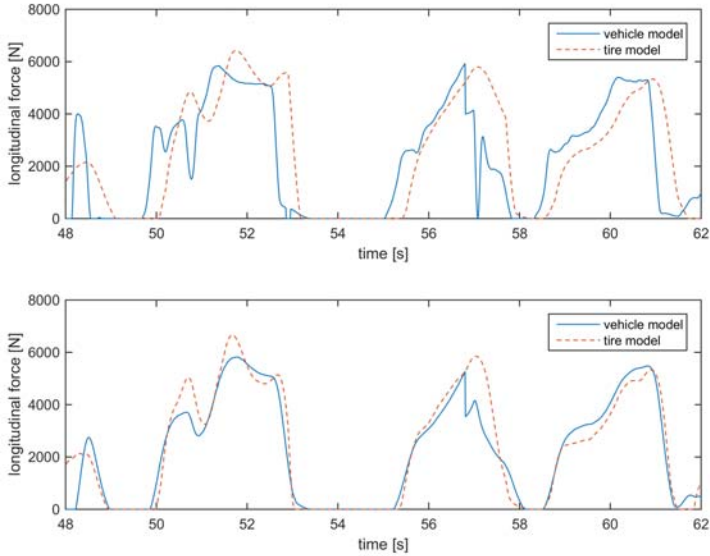


FIGURE 4.3: The forces from both the vehicle and tire model. In subplot one, the wheel speed is filtered harder than engine torque, leading to a delayed difference between the vehicle and tire model. With the same filter values, used in subplot two, the two estimated forces match better.

ground by using two different radii. A radius difference of 3 cm would be very large if considering a tire pressure drop, but could be possible when changing between wheels. In the second subplot, the longitudinal force calculated from a tire model is presented. The two different masses correspond to a vehicle with merely a driver and a vehicle with 5 persons, respectively.

4.3 Vehicle forces

There are several forces acting on a vehicle. The largest forces are generated between the tires and the ground because the tires are the only parts of a vehicle that have any physical contact with the surrounding world. While accelerating and braking longitudinal forces will arise and while cornering lateral forces will arise. The tires are responsible for all the forces that actually control the vehicle which makes them very important for good handling but also makes them hard to model. Beside these major forces there are also forces such as aerodynamic drag and rolling resistance acting on the vehicle.

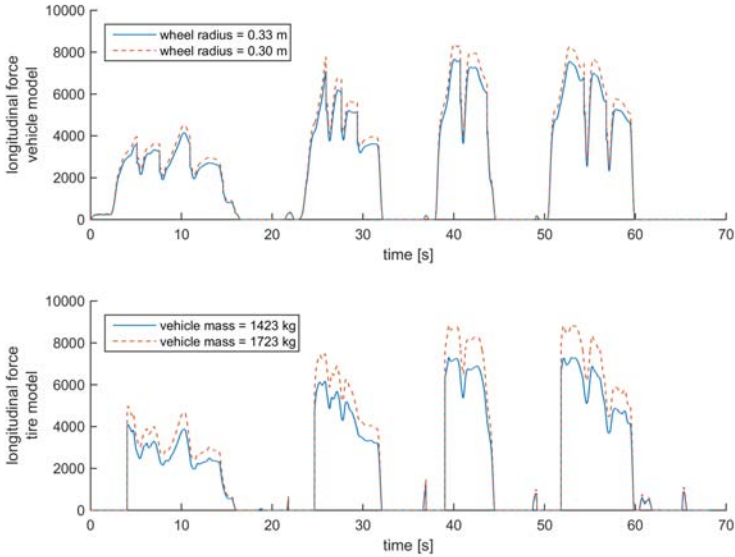


FIGURE 4.4: In the first subplot, the vehicle model force is plotted for two different wheel radius. In subplot two, the vehicle force is shown for two different vehicle masses.

The trick is to calculate all the forces into one total force that can be compared to the total force generated by the tires.

4.3.1 Vehicle force calculated from longitudinal acceleration

The simplest way of representing the force acting on the vehicle while accelerating is to use the acceleration and the mass of the vehicle and apply Newton's second law of motion:

$$F = m \cdot a \quad (4.1)$$

4.3.1.1 Estimating the longitudinal acceleration

For this method to be accurate an accurate estimation of the longitudinal acceleration is needed. Some vehicles have accelerometers installed for longitudinal measurements which makes it straight forward to calculate the force. If one of those aren't available the acceleration has to be calculated instead. This can be done by derivation of the vehicles velocity. The velocity of the vehicle can be obtained by measuring the speeds of

the undriven wheels. For an FWD vehicle this would be the rear wheels. To make the calculation more accurate the average speed of the two rear wheels is calculated before the derivation is done.

$$a_x = \frac{d}{dt} \left(\frac{w_{rl} + w_{rr}}{2} \right) \quad (4.2)$$

4.3.1.2 Estimating the losses

Two different losses are compensated for; losses from drag and losses from rolling resistance.

The drag force is calculated as:

$$F_D = \frac{1}{2} \rho v^2 C_d A \quad (4.3)$$

where:

- ρ is the density of air.
- v is the vehicle velocity.
- C_d is the drag coefficient.
- A is the cross sectional area.

The rolling resistance is calculated as in Equation 2.21.

4.3.1.3 Estimating the total vehicle force

The total amount of force acting on the vehicle thus becomes:

$$F_{vehicle} = m \cdot a + F_{drag} + F_{rollingresistance} + F_{roadgradient} \quad (4.4)$$

4.3.1.4 Complications

The main issue with this method is that it's based on longitudinal acceleration and longitudinal losses only. Hence it can only be used to estimate the vehicle forces when accelerating in a straight line. Although this is a big restriction it might be enough since acceleration in a straight line happens pretty often while driving.

A major hardship is to obtain a proper value for the longitudinal acceleration. If the vehicle doesn't have an accelerometer the acceleration calculated from the wheel speeds

need to be used. This immediately causes problems when the vehicle is accelerating on a gradient road. During an uphill acceleration, the actual force to accelerate the vehicle will be larger than the force calculated from Newton's second law. Driving downhill, the force will be smaller. This is because the earth's gravity isn't considered in the formula. When climbing a hill the vehicle force needs to include the force of the earth's gravitational pull as well. The same goes for then driving downhill, but now the force will instead help accelerating the vehicle. The force of the gravitational pull can be calculated if the angle of the vehicle relative the earths horizontal plane is known but this angle is hard to measure or estimate. Measuring it with an accelerometer won't work either. The accelerometer will give a better result since the force of gravity is affecting it in some way. This is because it's changing inclination together with the vehicle but it still won't give an acceleration that corresponds to the actual force acting on the vehicle. A solution to this would be to have another accelerometer measuring vertical acceleration of the vehicle but this is extremely uncommon.

The second parameter of Newton's second law is the mass which also is hard to estimate. The mass of the vehicle can vary several hundreds of kilos depending on passengers and load in the trunk. A Golf GTi has a curb weight of about 1350 kg. Hence, the varying weight will have a great impact on the force calculations. To counter this problem some kind of load detection needs to be available to set a new mass every time the vehicle is driven. This isn't something that is very common on vehicles today and thus a static mass of the vehicle needs to be set resulting in errors in the force calculations way too often.

Suppose that the force calculation from Newton's second law is correct. Still there are losses to be accounted for. They need to be calculated properly to be able to compare the vehicle force to the tire force. Looking at Equation 4.4, two different losses are compensated for. The rolling resistance is straight forward if the rolling resistance coefficient is known. The drag is a bit more complicated but should prove to be fairly accurate as well if the parameters are known. All in all, the results of these calculations won't be perfect and there are several more losses that can't be calculated in any good way.

4.3.2 Vehicle force calculated from engine torque

Another way of calculating the longitudinal force of a vehicle is to derive the actual torque that is applied to the shafts connected to the driven wheels. To calculate this the torque on the crank shaft can be used which is available as a signal on the CAN bus. The advantage of using the engine torque, instead of the acceleration of the vehicle, is

its independence of the roads gradient and losses such as wind drag and steering losses. The torque that is applied to the shafts will be directly proportional to the actual force generated by the wheels, regardless of how the gravitational pull and other losses are acting on the vehicle.

The formula for calculating the total torque on the drive shafts is simple:

$$T_{driveshafts} = T_{engineshaft} \cdot GearRatio \quad (4.5)$$

where the gear ratio is the speed ratio between the engine shaft and the differential housing:

$$GearRatio = \frac{\omega_{engine}}{\omega_{diffhouse}} \quad (4.6)$$

and finally the speed of the differential housing is the average speed of the left and right drive shafts:

$$\omega_{diffhouse} = \frac{\omega_{leftdriveshaft} + \omega_{rightdriveshaft}}{2} \quad (4.7)$$

The engine torque, engine speed and the drive shaft speeds (wheel speeds) are all signals commonly found on the CAN bus of a newer car. Important to notice is that these calculations do not consider any losses from the engine to the drive shaft. By combining Equations 4.5 & 4.6, it is seen that the power generated by the engine and the power outputted to the drive shaft are equal.

$$P = T_{driveshaft} \cdot \omega_{driveshaft} = T_{engineshaft} \cdot \omega_{engineshaft} \quad (4.8)$$

The torque will be split evenly between the two drive shafts, assuming an open differential, i.e. when the FXD is inactive. If the FXD is active the available torque on the drive shafts has to be redistributed according to the amount of torque being transferred through the FXD. This is important to consider if force calculations for a single wheel are to be done.

When the torque on each drive shaft is calculated the force acting on each tire is calculated by dividing that torque by the wheel radius:

$$F_{tire} = \frac{T_{shaft}}{R_e} \quad (4.9)$$

These forces can then be compared to the forces generated by the tire models for each tire.

Gear	Gear ratio
1	13.9284
2	8.5383
3	5.4378
4	3.7206
5	2.7666
6	2.1942

TABLE 4.1: Gear ratios for the Volkswagen Golf GTi Mk7

4.3.2.1 Gear ratio

Calculating the gear ratio with Equations 4.6 & 4.7 gives varying results. Both the engine speed and wheel speed signals are noisy. In the gear change moment it will take some time for them to stabilize again resulting in long times of faulty force calculations.

On newer cars it's common to have a signal on the CAN bus that contains information of which gear is active at the moment. By knowing this the gear ratio can be set without any calculations because the gear ratio for each gear is known for a specific vehicle. For the Golf GTi the gear ratios can be seen in Table 4.1. A graph of the calculated and predefined gear ratio can be seen in Figure 4.5. It can be seen that the calculated signal is much slower than the predefined one. It's also oscillating quite much which is bad because the gear ratio really is a static value purely depending on what gear is active.

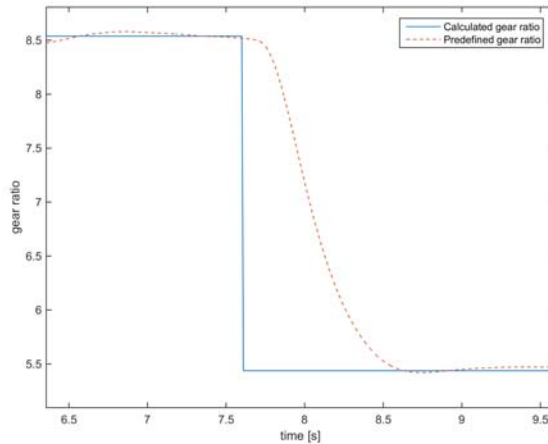


FIGURE 4.5: Calculated and predefined gear ratio in a gear change from 2nd to 3rd gear.

4.3.2.2 Transfer losses

There are several factors that affect how much of the engine torque that actually becomes available on the drive shafts. There are several losses in a drive line. Friction and rotating masses within the drive line are the main contributors. Some torque are also lost accelerating the mass of the wheel itself.

$$T_{driveshaft} = T_{driveshaftwithoutlosses} \cdot \eta_{friction} \cdot \eta_{rotatingmass} - T_{wheelacceleration} \quad (4.10)$$

$\eta_{friction}$ is just a scalar factor. The frictional losses are very dependent on the design of the drive line. This means that the losses will differ between vehicles and that this factor needs to be calculated for each specific car model.

The losses due to the acceleration of the drive shaft is also included in the rotating mass scaling factor. $\eta_{rotatingmass}$ is modeled as [11]:

$$\eta_{rotatingmass} = \frac{1}{1 + x \cdot gearratio^2} \quad (4.11)$$

The efficiency gets worse as the gear ratio gets higher since there will be more rotating mass in low gears. The variable x in Equation 4.11 models how much of an impact the gear ratio should have on the efficiency. Just as the frictional losses this loss is also dependent on the design of the drive line. Thus the factor multiplied with the gear ratio needs to be decided for each specific car model.

To calculate $T_{wheelacceleration}$ requires some more steps. Each wheel connected to a driven shaft has its own moment of inertia which will be accelerated if enough torque is applied. The amount of torque needed to accelerate the wheel depends on its moment of inertia and the angular acceleration:

$$T = a \cdot I \quad (4.12)$$

The moment of inertia is the wheels radius squared and integrated over the mass.

$$I = \int r^2 \cdot dm \quad (4.13)$$

Assuming that a wheel has the shape of a solid cylinder with equal amount of density throughout, the moment of inertia for a wheel can instead be described as:

$$I = \frac{r^2 \cdot m}{2} \quad (4.14)$$

In the same manner, this applies for the actual drive shafts as well but as was said earlier this loss is included in the scalar factor describing the frictional losses.

The angular acceleration is calculated in the same manner as in Section 4.3.1.1 but now for the front left and right wheel separately.

4.3.2.3 Complications

The main issue with this method is the overall uncertainty of it. For example, the engine torque obtained from the CAN bus isn't measured with a torque sensor on the crankshaft but rather is a calculated value from the engine control unit. The engine control unit calculates the torque with the help of several engine parameters and even if it's close most of the times there are moments when it isn't quite right. When doing a sudden acceleration that's aggressive enough to make the vehicle shift down some gears, a so called kickdown, the torque reading will be faulty.

This method won't work during shifting because the link between the engine shaft and the drive shafts will be lost or affected while the clutch and transmission are working to shift gear. To avoid this trouble the vehicle force estimation simply needs to be paused as soon as the start of a gear shift is detected.

4.3.2.4 Verification

Since the reliability of the method is uncertain it needs to be verified in some way. This was done with test data from a driving session where the vehicle was equipped with torque sensors mounted on the drive shafts. By comparing the results from the calculated torque values to the measured values the functionality of the method can be verified. Further on some basic tuning of the efficiency coefficients can be made. In Figure 4.6 the verification can be seen.

4.3.3 Choosing vehicle model

Two different models for estimating the vehicle force have been presented. One is based on calculating the force using Newton's second law. This model can be divided into two sub-models since the vehicle acceleration can be calculated by derivation of the undriven wheel speed or measured with an accelerometer. The other model uses the engine torque to calculate the vehicle force. Thus, the vehicle force can be acquired in three different ways and it's of course desired to use the most accurate model. When driving in a straight line on a flat road these three models will result in almost the same force, as can be seen in Figure 4.7. The engine torque model will drop below the other models

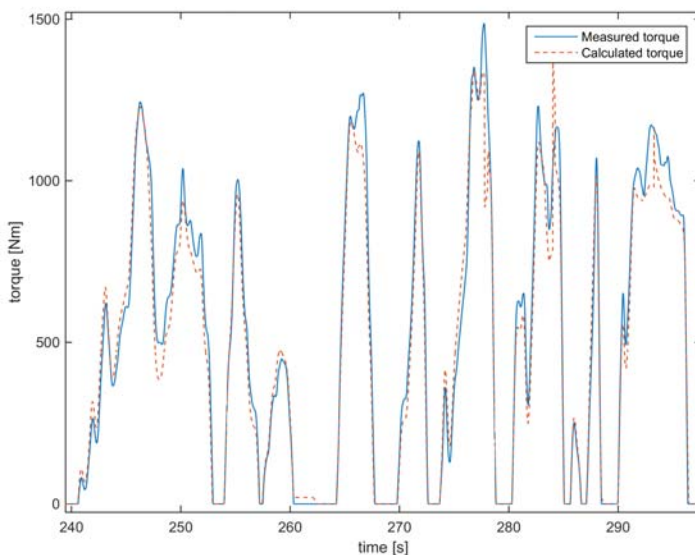


FIGURE 4.6: Measured and calculated torque on the left drive shaft from a vehicle equipped with torque sensors on the drive shafts.

while shifting gear since the engine is disconnected from the wheels while doing so. This is something that has to be considered and will be further explained in Section 4.6.3.2.

The models will differ more when cornering, as can be seen in Figure 4.8. Neither the method with acceleration calculated from the undriven wheel speed nor the measured acceleration from the accelerometer will be accurate while cornering. This is because both methods for acquiring the vehicle acceleration is for longitudinal acceleration only. The undriven wheels are in this case the rear wheels and since these can not turn, only the longitudinal acceleration is represented. The same goes for the accelerometer. Only the longitudinal part of the acceleration is measured. The actual acceleration of the vehicle while cornering is a combination of longitudinal and lateral acceleration. The result of all this is that the force from the acceleration-based vehicle models gets too low when cornering.

A solution to this could be to measure both the longitudinal and lateral accelerations with accelerometers and calculate the total acceleration of the vehicle. Unfortunately it's not that easy. When using both longitudinal and lateral acceleration of the vehicle the tire models must be able to account for both longitudinal and lateral force which is hard to model. More on this in Section 4.4.

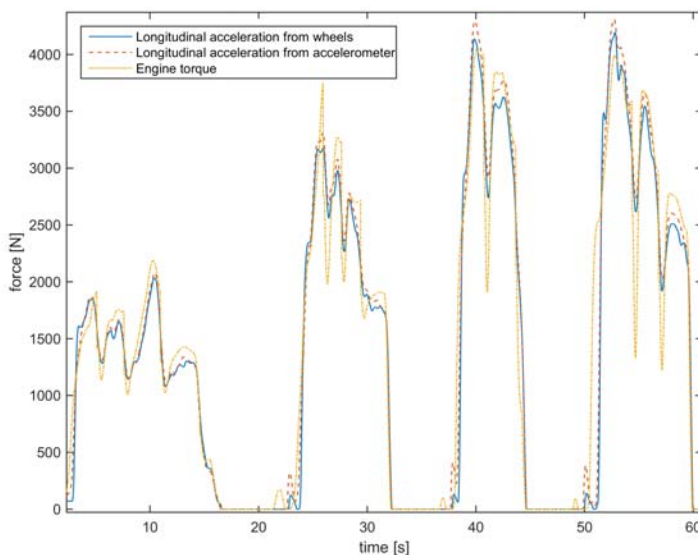


FIGURE 4.7: The vehicle force for the three different models while driving in a straight line on a flat road.

It gets even worse when driving on a road that's hilly, as can be seen in Figure 4.9. While driving uphill or downhill the longitudinal acceleration from both the calculations and the accelerator measurements will be wrong. The drive session shown is uphill, hence the force will be too low since the force needed to counter the force of gravity isn't considered. When cornering both acceleration-based models were almost equally faulty at all time. When driving on a hill there's a difference between them. This is because the model based on undriven wheel acceleration won't consider the force of gravity at all. The model based on the accelerometer will consider it to some extent since the accelerometer will incline with the vehicle, although, it won't be right.

The acceleration-based vehicle models have been discussed a lot so far. The model based on engine torque hasn't been mentioned much at all and it has even been implied that this one is correct when the acceleration-based models are falling behind. This is because it really is a good model that fills its purpose. It's not affected by hills and it's not as severely affected by cornering as the acceleration-based models are. The force will always be applied in the longitudinal direction of the tire, hence it works good to match this with a longitudinal tire model. The main problem is the fact that the slip ratio calculation will be a bit off while cornering since lateral velocity isn't considered

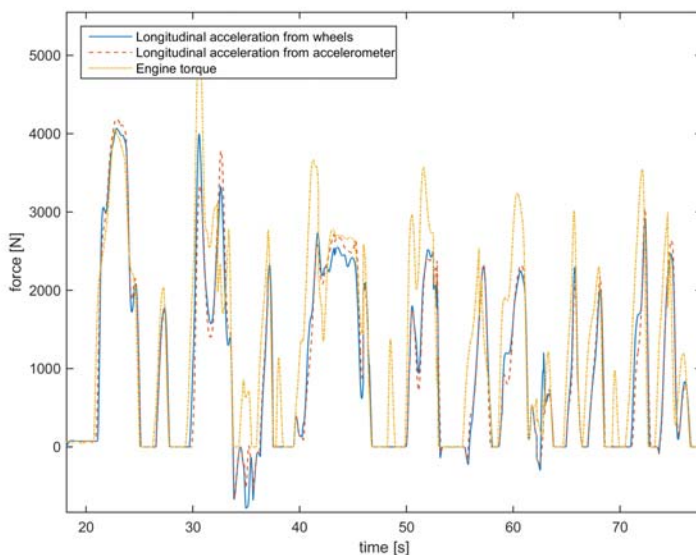


FIGURE 4.8: The vehicle force for the three different models while driving along a track with several corners.

but this is solved later on in Section 4.5.3.

All in all, the obvious choice is the engine torque-based vehicle model.

4.4 Tire forces

The characteristic of a tire is very complex, which makes the actual force generated to the vehicle difficult to obtain. As was shown in the theory part, Section 2.3, there are several tire models that can be used, everyone of them with different properties.

A tire can generate both longitudinal and lateral force. It's quite easy to create a tire model that considers both these forces, but the hard part is to acquire all the input signals to the model in real time while driving. The signals to model the lateral force are especially hard to obtain. These signals are the slip angle and the lateral tire stiffness. Since these are so hard to calculate only the longitudinal part of a force model is used. The main dynamic parameters of a longitudinal tire force model (except for the Magic formula) includes the slip ratio, κ , normal force, F_z , and the tire/road friction coefficient,

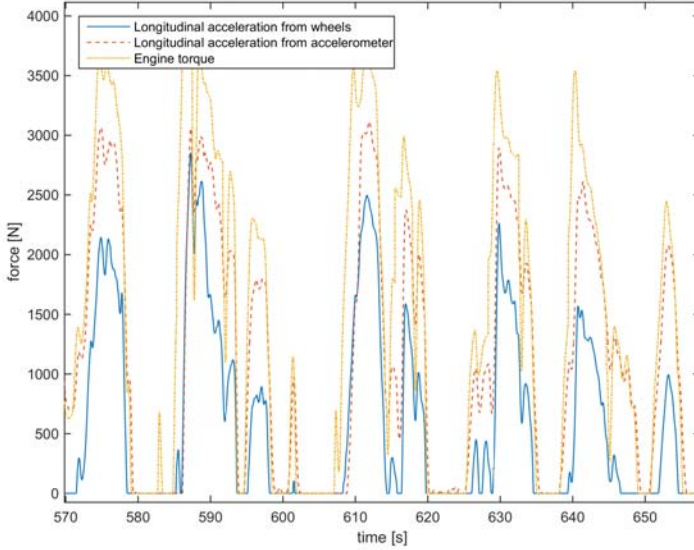


FIGURE 4.9: The vehicle force for the three different models while driving along a track with several corners and hills.

μ . A fourth, less dynamic parameter is the longitudinal tire stiffness, C_x .

$$F_{tire, longitudinal} = f(\kappa, Fz, \mu, C_x) \quad (4.15)$$

The slip ratio is calculated from the wheels difference in angular and forward velocity as seen in Equation 2.22, the normal force is calculated from the weight of the vehicle and the changing weight distribution derived in Section 2.1.3, and the tire stiffness as explained in Section 2.2.4. Thereafter, the only dynamic parameter of the tire force equation becomes the friction coefficient. By choosing the correct μ , the force from the tire model will equal the force from the vehicle model. This calculation is done in a feedback manner, meaning that the tire force depends on the friction coefficient derived in the previous iteration.

4.4.1 Choosing a tire model

Four models were described in the theory part; Brush model, Dugoff model, Magic formula and a tire model created by Ola Nockhammar at BorgWarner Torque Transfer Systems AB, further on called the BW model.

The Magic formula was ruled out almost immediately since it's a too complicated model. The sheer amount of variables it depends on makes it really hard to make it adaptive enough. Some of them are hard to calculate and some of them are almost impossible to obtain. It's great for simulating a specific tire in a lab for example but using it in a real time vehicle environment will be too complex. Further on the model requires several trigonometric calculations which is hard to implement efficiently in C code that's supposed to run on a simple micro controller.

The other three models are more simple with fewer input parameters and above all their parameters are more easily available, like slip ratio and normal force. The Brush model and the Dugoff model are even too simple. The only available parameter to change the characteristics of the force per slip ratio curve is the longitudinal tire stiffness. The BW model on the other hand contains two degrees of freedom by introducing a second parameter to affect the inclination of the force per slip ratio curve. Hence, it's easier to model a tire correctly with this model. Another positive aspect is the fact that the model is made for longitudinal force estimation only. Thus, it doesn't need to be modified for longitudinal use only like the Brush and Dugoff models.

All in all, the BW model was the obvious choice for this work.

4.4.2 Tire model parameters for the BW tire model

In this section four of the model parameters that affect the BW tire model will be explained in more detail.

4.4.2.1 Tire stiffness

The tire stiffness is obtained by deriving the tire force generated per slip ratio for values around zero, i.e. the gradient of the force per slip ratio curve at zero slip ratio. The slip force curve for two different tire stiffnesses can be seen in Figure 4.10. The interpretation from this figure is that a tire's stiffness is an essential parameter to have in order to model the tire force correctly.

Unfortunately, a tire's characteristics is further complex, and cannot be explained by the tire stiffness as a parameter alone. Two different tires can have the same tire stiffness, but differing characteristics at larger slip ratio values. An example of this can be seen in Figure 4.11. Generally, tires with lower tire stiffness value have higher ξ , hence resulting in even lower forces for higher slip ratio values. Once again this is a good reason to use the BW tire model since ξ can be modified in this model.

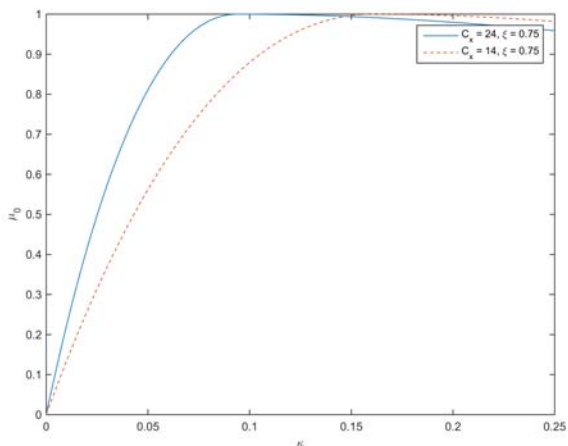


FIGURE 4.10: Normalized force from the BW tire model per slip ratio for two different tire stiffnesses. $\mu = 1.0$.

The tire stiffness for a certain tire should theoretically be the same for different road surfaces. Nevertheless, testing has shown that the actual inclination of the force per slip ratio curve for small slip ratios can differ for different road surfaces. The tire stiffness therefore has to be compensated accordingly depending on the roads friction coefficient.

4.4.2.2 Slip ratio

As seen most force per slip ratio figures, the maximum force will be generated at a specific slip ratio and will thereafter decrease with an increasing slip ratio. If the tire model doesn't capture this force peak at the correct slip ratio value, it will become very difficult to match the tire model force with the calculated vehicle force. The slip ratio value during a real driving sequence is usually rather small (maximum force is generally obtained at a slip ratio $\geq 12\%$), which means that small variances in the slip ratio calculations will have a large impact on the resulting force.

In order to calculate the slip ratios of the two front wheels, the four wheel speeds are gathered from the vehicles CAN bus. These signals generally include quite a lot of measurement and/or process noise which will lead to inaccurate slip ratio calculations, as can be seen in the first row of Figure 4.12. In order to overcome this noise and capture the actual value, the signals are run through a low pass filter. The wheel speeds will, even after filtering, have an oscillating attribute. When these oscillations from the front and its respective rear wheel are not synchronized and of different magnitude, the

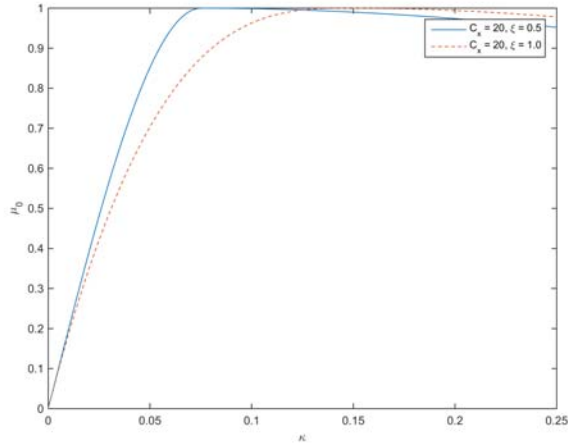


FIGURE 4.11: Normalized force from the BW tire model per slip ratio for two different ξ values. $\mu = 1.0$.

calculated slip ratio will have rather large variation compared to its real value. This can be seen in the second row of Figure 4.12, where the wheel speeds are run through a relatively slow low pass filter, i.e. a low pass filter with a low cutoff frequency. Most of the measure and/or process noise are removed, but due to the characteristics of the wheel speed sensor and its design, the signal will still oscillate with a frequency that is proportional to its angular velocity. To minimize the error from the oscillations, the wheel speeds are filtered with a lower cutoff frequency, which can be seen in the third row of Figure 4.12. Another concrete problem that arises when calculating the slip ratio, is that the radius for each wheel on a vehicle can be different, e.g. when the air pressure of a tire drops slightly over time. The wheel speed from the CAN bus will in this case be wrong, leading to an offset in the slip ratio calculations. Methods to calculate difference in wheel radii already exists, therefore the wheel radii are assumed to be known at all times.

4.4.2.3 Normal force

The amount of longitudinal force (neglecting lateral forces) generated from a tire depends on the normal force acting on the tire. The force generated by a tire is assumed to be linearly proportional to the normal force on the tire:

$$F_x = F_z \mu_0 \quad (4.16)$$

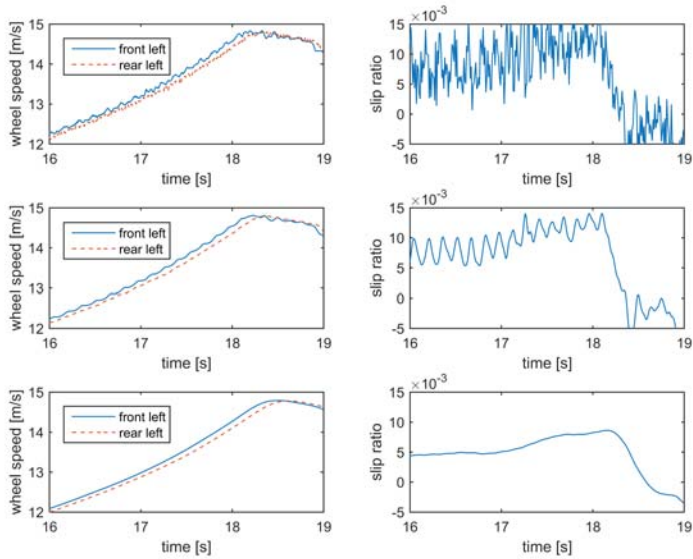


FIGURE 4.12: Wheel speeds and its calculated slip ratio. No filter of the wheel speeds are done in subplot one and two, resulting in much noise. Subplot three and four include a slow low pass filter where oscillations are present. Subplot five and six show the result when the wheel speeds are filtered with a harder low pass filter, giving a more stable slip ratio.

where the normalized force μ_0 , never can exceed the friction coefficient between the tire and the road:

$$\mu_0 \leq \mu \quad (4.17)$$

It is therefore important to know the loaded weight on each tire at every instant. This is done by the dynamic weight distribution calculations explained in Section 2.1.3. These calculations are rather simplified, where the difference in chassis stiffness between front and back is not considered. These chassis stiffnesses are vehicle specific and hard to estimate.

This means that the maximum longitudinal force obtained by either the vehicle model or the tire force model, can never be larger than the normal force multiplied by the tire/road friction coefficient, which can be helpful to rule out unreasonable values.

4.4.2.4 Friction coefficient

The final dynamic parameter that affects the tire force model is the friction coefficient between the tire and the road. The friction coefficient limits the normalized force that can be generated through the tires, which means that the friction coefficient and the normal force, $F_z\mu$, limits the amount of longitudinal force possible to acquire. How different μ affects the force/slip curve for the BW tire model can be seen in Figure 4.13. For a certain slip ratio value, different normalized force values will be acquired for the variant friction coefficient. It should also be noted in the figure that the derived force will not differ greatly depending on the friction coefficient at low slip ratio values. It is therefore desired to have a somewhat larger slip ratio value before the estimating the friction coefficient value. In other words, the normalized force should be closer to the frictional limit in order to acquire a more correct friction coefficient.

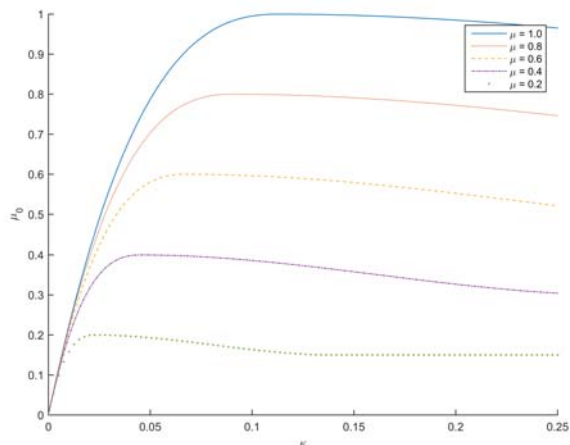


FIGURE 4.13: Normalized tire model force per slip ratio for different μ values.

4.5 Fitting the tire model

It is, as seen Section 4.4, very important to know the parameters that affect the force derived from the tire model. Slip ratio and the normal force is derived by using CAN signals from the vehicle and the friction coefficient is the parameter that should be approximated. The tire stiffness on the other hand is harder to approximate with good accuracy. The definition is, as mentioned earlier, the gradient of the slip/force curve

around zero slip ratio, which means that the tire stiffness should preferably be approximated at small slip ratio values, where the gradient is relatively constant. The force per slip ratio between 0 % and 2 % slip ratio can be seen in Figure 4.14. The figure shows that the variance of the force per slip ratio is rather large around the approximated line at $C_x = 24$, which would make a dynamic tire stiffness estimator unreliable. It should be noted that the driving sequence used in Figure 4.14 includes a lot of lateral acceleration, which adds to the C_x variance. Even though, it shows the difficulties of approximating the tire stiffness for real driving sequences.

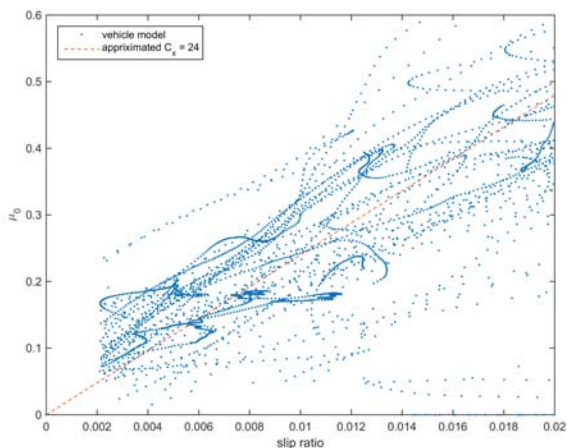


FIGURE 4.14: Force per slip ratio for lower slip ratio values which can be used to estimate the tire stiffness. Large variations create difficulties for a stable approximation.

Due to the difficulties to estimate the tire stiffness some experimenting have been made to fit tire model parameters during test driving. The problem with this solution is that static tire model parameters would be chosen for a certain driving sequence instead of having a dynamic solution that works for all kinds of tires.

It was also found during testing that the tire stiffness for the same set of tires changes depending on the friction coefficient between the tire and the road. The tire stiffness will therefore be interpolated between two different tested tire stiffness values. This interpolated formula will depend on the tire/road friction coefficient.

4.5.1 Winter tires

Test driving has been done on a set of winter tires on both asphalt and ice/snow. In Figure 4.15 the force per slip ratio can be seen during a simple acceleration run on

asphalt. Here all data points for the drive session are displayed which results in several faults. For example the data points with high force at zero slip ratio is when launch control is activated, i.e. the engine generates torque but the vehicle stands still. These data points can't be used when estimating the friction coefficient and those together with many other are removed when the estimator is active. More on this in Section 4.6.3.

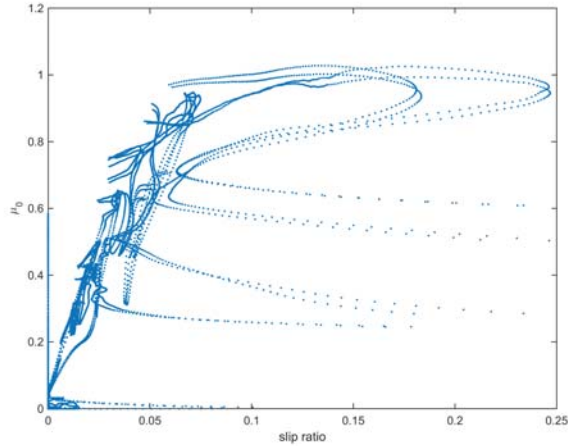


FIGURE 4.15: Normalized force per slip ratio for acceleration in a straight line with winter tires on asphalt. All measured values from the driving sequence is used.

For now we assume that only valid data points are displayed. The same drive session with faulty data points removed can be seen in Figure 4.16. Fitting a tire model to these data points are a much easier task and the fitted tire curve can also be seen in this figure.

The tire model parameters that were fitted to the data and the friction coefficient became:

$$\begin{aligned}
 C_x &= 24 \\
 \xi &= 0.9 \\
 \mu &= 1.0
 \end{aligned}
 \tag{4.18}$$

In Figure 4.17 the force per slip ratio can be seen during a driving sequence on ice/snow. The fitted tire curve can be seen in this figure as well. This driving sequence was made on a track with corners and is not merely an acceleration in a straight line. The effect

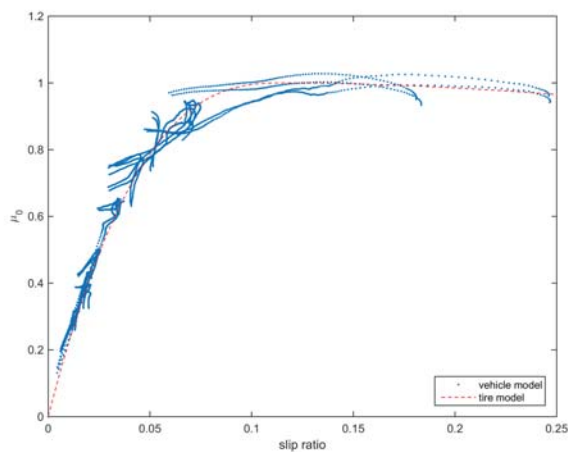


FIGURE 4.16: Normalized force per slip ratio for acceleration in a straight line with winter tires on asphalt. Only values that fulfill the conditions in 4.6.3 are used.

of this is more variance in the vehicle force calculation compared to the result in Figure 4.16.

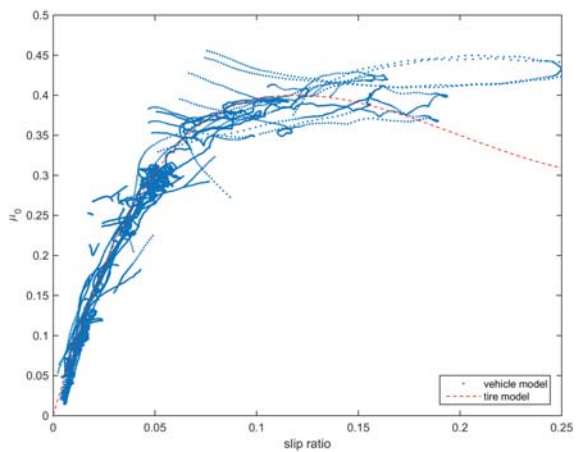


FIGURE 4.17: Normalized force per slip ratio for a track run on ice/snow with winter tires.

The parameters for the fitted tire model and the friction coefficient for the ice driving sequence became:

$$\begin{aligned} C_x &= 9.5 \\ \xi &= 0.9 \\ \mu &= 0.4 \end{aligned} \tag{4.19}$$

As mentioned earlier it can be seen that the exact same winter tire differs a lot in stiffness depending on road conditions. To get the correct tire stiffness for different friction coefficients, a first order polynomial was interpolated for the different C_x and μ in Figure 4.18 & 4.19. This polynomial became:

$$C_x = 25\mu - 1 \tag{4.20}$$

4.5.2 Summer tires

Test driving has also been done on a set of summer tires on asphalt. The tires used were low-profile tires which generally means high stiffness, i.e. low slip ratio values are needed to acquire high longitudinal force, which can be seen in Figure 4.18. The data acquired from this driving sequence does not include a lot of slip ratio around the peak slip ratio, much due to the high stiffness and good grip from the low-profile tires. It is only in the first gear that the slip ratio actually exceeds this peak in force which is assumed to be at slip ratio $\approx 6\%$.

The fitted tire curve can also be seen in Figure 4.18 and there parameters for that driving sequence became:

$$\begin{aligned} C_x &= 38 \\ \xi &= 0.7 \\ \mu &= 1.15 \end{aligned} \tag{4.21}$$

Due to lack of testing with summer tires on ice/snow, no correct linearization can be made between the different μ and C_x . The first order polynomial therefore is assumed to have the same characteristics as for the winter tires:

$$C_x = 34\mu - 1 \tag{4.22}$$

Note that this equation should be further tested before accepted as a way to calculate the tires stiffness. Due to the fact that there are differences in the characteristics of

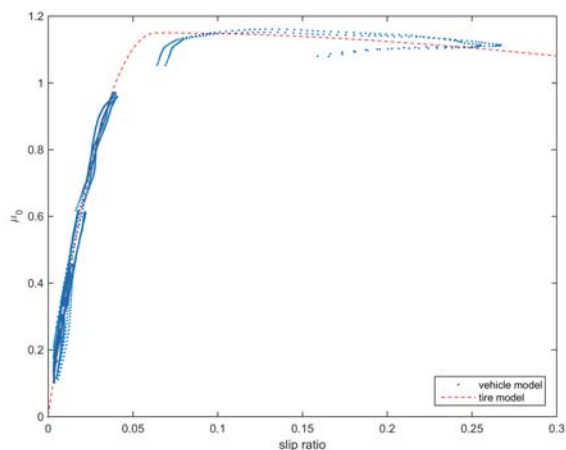


FIGURE 4.18: Normalized force per slip ratio for acceleration in a straight line with summer tires on asphalt.

winter and summer tires, this approximation should not be taken as a credible solution, but merely serve as a guideline due to previous experiments.

4.5.3 Lateral acceleration compensation

The force per slip ratio curves seen in Figure 4.16 & 4.18, that were used to fit the tire model parameters, are derived from data acquired from a test run when acceleration was done in a straight line. This means that no lateral forces are acting on the tires, which is a very ideal condition and won't happen very often in real life driving. When a vehicle is turning, it will also have a slip angle between the tire's heading and pointing direction. When slip angle is present, the amount of longitudinal force actually generated per slip ratio will become less, see the curves for different slip angles in Figure 2.9. However, slip angle is a parameter which is hard to approximate, and assumed to be unknown in this report. A signal that is correlated to slip angle is the lateral acceleration, which means that it is most likely that lateral acceleration is present when a slip angle is. Simple put, when there is lateral acceleration present the calculated slip ratio needs to be lowered. An approximation for the new slip ratio that is to be used is derived by:

$$\kappa_{a_y \text{ compensated}} = \frac{\kappa}{1 + a_y \cdot \beta} \quad (4.23)$$

where β is a scaling factor that decides how much of an impact the lateral acceleration should have. In Figure 4.19, two different force per slip ratio curves can be seen for a driving sequence which includes cornering at high velocities, meaning that slip angle as well as lateral acceleration is present. The data is taken from a driving sequence using the same winter tires as seen in Figure 4.16, and therefore also uses the fitted tire model parameters from Equation 4.18. In the first subplot of Figure 4.19, no compensation for lateral acceleration is done, while the data in the second subplot uses the approximated slip ratio derived by Equation 4.23 with $\beta = 0.15$.

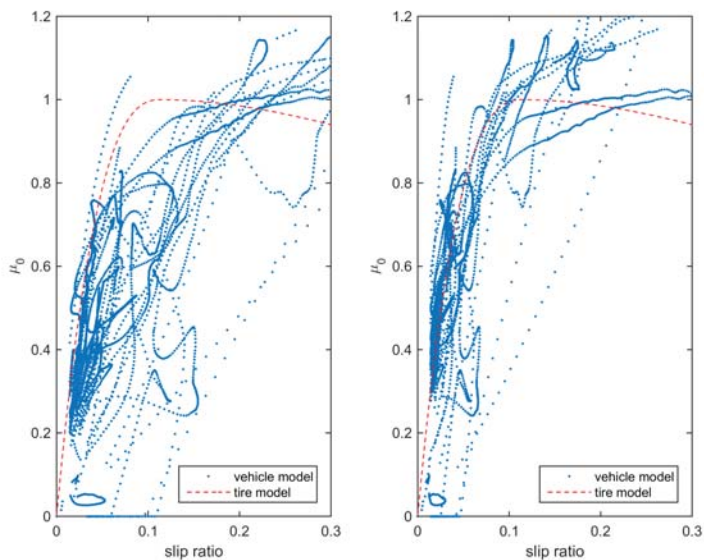


FIGURE 4.19: Normalized force per slip ratio for a fast track run. The first subplot shows the result without lateral acceleration compensation. In subplot two, the slip ratio value is compensated depending on the lateral acceleration.

It can be seen that the result from the second subplot corresponds better to the fitted tire model parameters that were acquired on a straight line acceleration. Even after the slip ratio has been compensated for, it is seen that the resulting force per slip ratio values have much higher variance than the acceleration run showed. This once again shows the difficulties in modeling different possible driving sequences with good accuracy.

4.5.4 Tire mode selector

The two different fitted tire models presented in 4.5.1 & 4.5.2 can result in very differing forces at the same slip ratio value. It's therefore important to know if the vehicle is equipped with winter or summer tires in order for the system to work. It should also not be a necessity for the driver to specify what kind of tires that are used. The tire mode selector consists of an algorithm that finds the set of tire model parameters that matches the force from the vehicle model with the smallest error. The algorithm calculates the force difference between the respective set of tire parameters and the vehicle model. It is low pass filtered to eliminate sudden changes that shouldn't affect the choice of tire parameter set. The filtered result can be seen in Figure 4.20. Winter tires are used in the first subplot, where the difference between the summer tires and vehicle model is seen to increase over time. In the second subplot, summer tires are used instead, and the difference between the winter tire and vehicle model is seen to decrease as time passes. The tire mode selector can be seen in Figure 4.21.

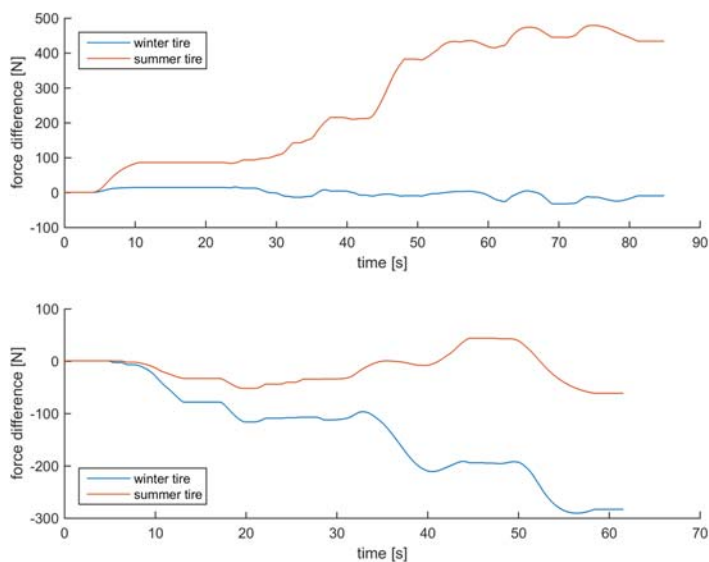


FIGURE 4.20: The force difference between two set of tire model parameters compared to the vehicle model force. This difference between the two models are low pass filtered. First subplot shows the result from a driving sequence using winter tires and the second subplot shows the result from a driving sequence with summer tires.

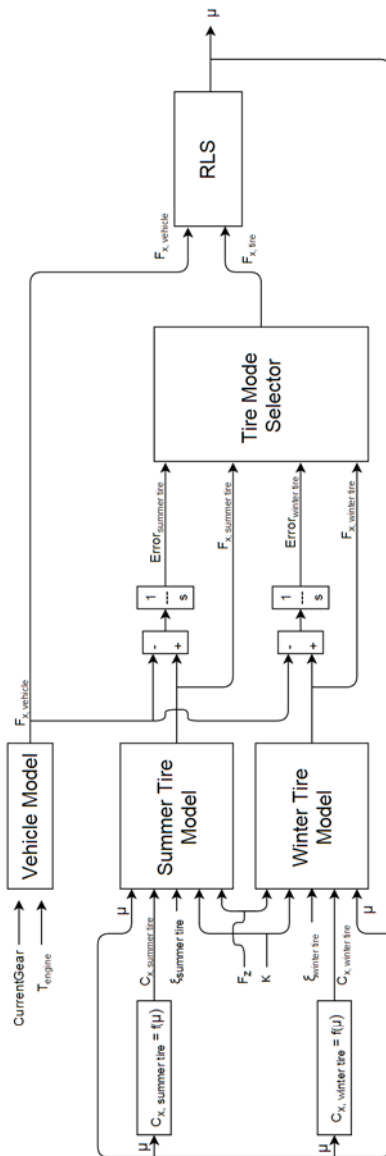


FIGURE 4.21: The extended friction estimator with tire model selector and adaptive longitudinal tire stiffness coefficient.

4.6 Estimating the friction coefficient

The extended friction estimator with tire model selector and adaptive longitudinal tire stiffness coefficient can be seen in Figure 4.21. The aim of the friction estimation is, as mentioned earlier, to choose the correct friction coefficient so that the forces from the two different models become equal. In other words, choose the μ that enables:

$$F_{vehicle} = F_{tire} \quad (4.24)$$

This relation, and therefore also a friction coefficient, could theoretically be obtained at every instance when new CAN packages are available. This would lead to a rapidly changing friction coefficient which wouldn't reflect the actual tire/road friction. Instead of approximating a new friction coefficient at every moment, a least square fitting method is used to find the friction coefficient. The goal of such a method is to find the friction coefficient that provides the smallest error between the two models over a certain amount of time.

It could be possible to estimate two different friction coefficients, one for each of the driven tires and its road contact. This means that a split- μ scenario could be detected. The trade-off to estimating two different friction coefficients instead of one, is that variances between the models would result in larger estimation error. It has been chosen that a more stable friction estimation is preferred rather than being able to detect two different friction coefficients. The vehicle and tire model forces are here on after the combined force from the two driving tires.

$$\begin{aligned} F_{vehicle} &= F_{vehicle,left} + F_{vehicle,right} \\ F_{tire} &= F_{tire,left} + F_{tire,right} \end{aligned} \quad (4.25)$$

4.6.1 Least square fitting

The general idea of a least square fitting method is to minimize the sum of the squares between a theoretical model and observed data.

$$y(k) = \phi(k) \cdot \theta + v \quad (4.26)$$

where y is the observed data, $\phi(k) \cdot \theta$ the theoretical model and v the error. The cost function that should be minimized becomes:

$$V(\hat{\theta}, k) = \frac{1}{2} \sum_{i=1}^k \lambda^{k-i} \left(y(i) - \phi(i) \cdot \hat{\theta} \right)^2 \quad (4.27)$$

Due to the fact that new data is acquired continuously, these least square approximations would need to be executed at every time step, creating unreasonable amount of computations. Hence, a modification of the least square fitting is used which recursively takes previous results into account.

4.6.2 Recursive least square fitting

The recursive least square (RLS) fitting method is defined as:

$$L(k) = \frac{P(k-1)\phi(k)}{\lambda + \phi^T(k)P(k-1)\phi(k)} \quad (4.28)$$

$$P(k) = \left(1 - L(k)\phi(k)\right) \frac{1}{\lambda} P(k-1) \quad (4.29)$$

$$\hat{\theta}(k) = \hat{\theta}(k-1) + L(k) \cdot v(k) \quad (4.30)$$

where the error is:

$$v(k) = y(k) - \phi^T(k)\hat{\theta}(k-1) \quad (4.31)$$

L and P defines how much the next update of θ should rely on the error. A larger L takes the error into account more, while a smaller number makes the update rely on the old θ value more. The forgetting factor, λ , is defined by the user and basically describes how many previous values to consider when calculating a new θ .

However, this method can only be applied to linear system, and a tire force, $F_{tire} = f(\kappa, F_z, \mu, C_x)$, is not linear. To able to use the RLS, the function has to be linearized. To accomplish this, the derivative of the force as a function of μ is defined as:

$$\frac{\partial F}{\partial \mu} = \frac{\partial f(\kappa, F_z, \mu, C_x)}{\partial \mu} \quad (4.32)$$

which describes how much the force will increase dependent on μ . The force in that linearized region thereafter becomes:

$$F_{vehicle} = \frac{\partial F_{tire}}{\partial \mu} \cdot \mu \quad (4.33)$$

This function now has the same form as Equation 4.26, which means that the RLS method in Equations 4.28-4.31 can be used. The RLS with the parameters related to this work is:

$$L(k) = \frac{P(k-1) \frac{\partial F_{tire}(k)}{\partial \mu}}{\lambda + \frac{\partial F_{tire}(k)}{\partial \mu} P(k-1) \frac{\partial F_{tire}(k)}{\partial \mu}} \quad (4.34)$$

$$P(k) = \left(1 - L(k) \frac{\partial F_{tire}(k)}{\partial \mu}\right) \frac{1}{\lambda} P(k-1) \quad (4.35)$$

$$\mu(k) = \mu(k-1) + L(k) \left(F_{vehicle}(k) - F_{tire}(k)\right) \quad (4.36)$$

The friction coefficient value is updated at every time step and depends on its own value, the error between the vehicle and tire model, and the number L describing how much to rely on the error. $\frac{\partial F_{tire}}{\partial \mu}$ becomes larger for slip ratios close to the peak force, which means that a larger change of μ is possible at that point. The forgetting factor, λ , is usually a value in the region $[0.9, 1)$, where a larger forgetting factor means that older values are considered more, resulting in slower changes of μ . The choice of λ affects the changing friction coefficient greatly. A value very close to 1 will generate a much more stable value for μ , while a slightly smaller number reacts faster to changes in the road condition.

4.6.3 When to estimate the friction coefficient

It would be desirable to be able to estimate the friction coefficient in every instant while driving in order to capture a change in the road condition as fast as possible. Unfortunately there exist many challenges during most driving sequences that have to be considered. During some situations, neither the vehicle nor the tire model are shown to model anything close to reality. These situations need to be identified so that the RLS fitting method does not update the estimated friction coefficient value. This means that the friction coefficient value will not be continuously updated throughout every driving sequence and that sudden changes of the tire/road friction can be missed.

4.6.3.1 Limitations due to slip ratio

There are a couple of driving sequences that affect the slip ratio in such a way that the forces cannot be modeled correctly. When braking, the slip ratio can no longer be calculated correctly since there's no braking torque signals available. During cornering, the front wheels will be turned creating a lateral force and a yaw rate. The rear, which doesn't have any positive cornering effect, will follow the front wheels but in a smaller radius, leading to a lower velocity. This difference in velocity between the front and rear wheels will result in a slip ratio that is non proportional to the amount of force generated at the tires. This phenomena will be larger when cornering at low velocities, due to the fact that a smaller lateral force is acting, and therefore not pushing the rear axle to a larger radius. This large slip ratio due to cornering can be seen in Figure 4.22. At around 20 s and after 30 s, the vehicle is turning at a low velocity. This results

in a large slip ratio estimation seen in the first subplot, which exists without adding a positive longitudinal force.

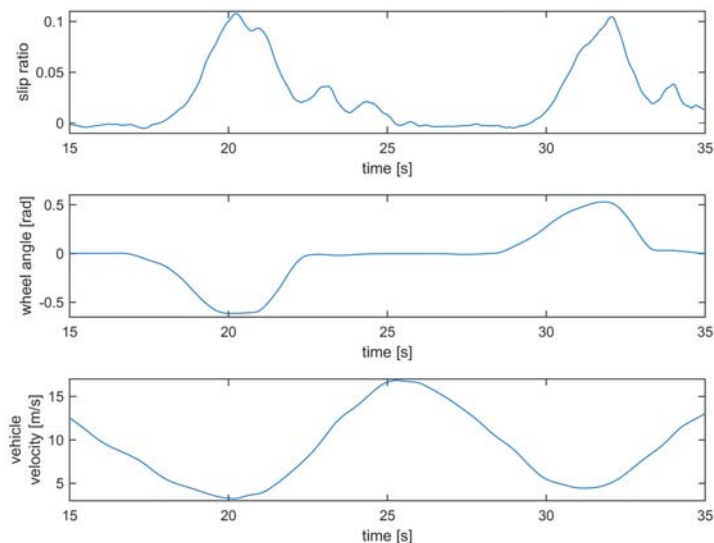


FIGURE 4.22: The slip ratio, wheel angle, and vehicle velocity for a driving sequence. The derived slip ratio is incorrect when the wheel angle is large and the vehicle velocity is relatively low.

Another driving scenario that creates a misleading slip ratio is during acceleration from standing still, which can be seen in Figure 4.23, at around 2 s and 24 s. When the acceleration begins, the front wheels will start to turn slightly ahead compared to the rear wheels. The percentage difference between the two wheels will become large due to the low velocity, leading to an unreasonable high slip ratio. The same phenomena can also be seen in Figure 4.23 right before the vehicle comes to a stop, at around 22 s.

Limitations has to be set so that the RLS fitting method does not update the friction coefficient during these scenarios when the calculated slip ratio gives an unreliable result.

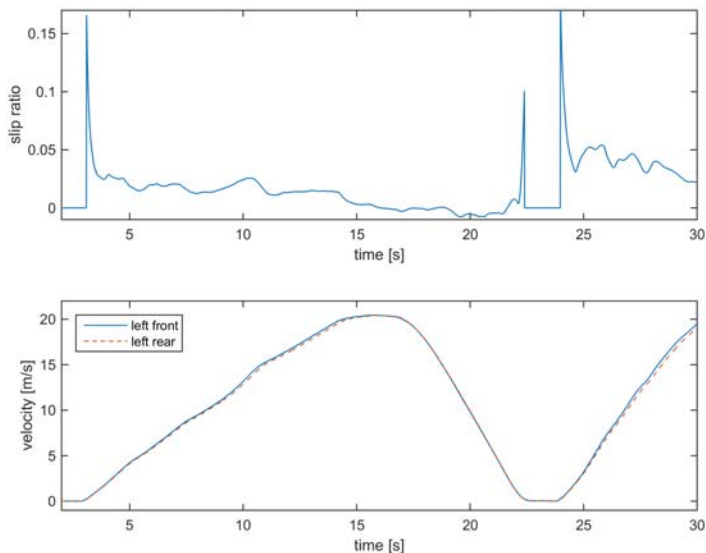


FIGURE 4.23: Large erroneous slip ratio values are seen when a vehicle acceleration begins as well as when it comes to a halt.

4.6.3.2 Limitations due to gear shifts

When a vehicle engages the clutch prior to a gear change, there will be no torque transferred from the engine to the wheels. Due to filtering and differences between various signals, the force losses in the different models will be different. This can be seen in Figure 4.24, where gear shifts appear at around 54.5 s and 57 s.

Due to this disturbance during the gear shifts, the RLS fitting method should not be updated during a certain amount of time after a gear shift engages. An updated friction coefficient can therefore not be calculated during this period.

4.6.3.3 Limitations due to low forces

Another limitation that adds to the restrictions when the friction coefficient shouldn't be updated is when the total force acting on the vehicle is too low. During this period of time, when the normalized force is far from the friction coefficient limit, it is very hard to approximate the actual value of the friction coefficient. The reason for this is that the force from the tire model changes less per μ for low forces, which can also be seen

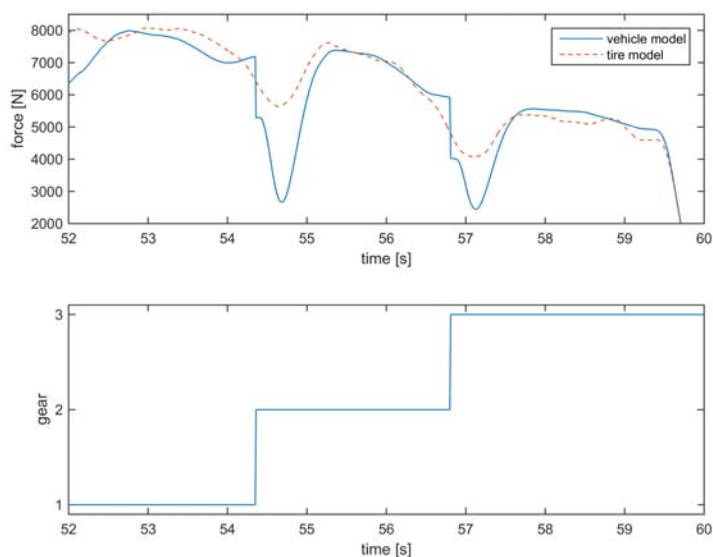


FIGURE 4.24: Vehicle and tire forces differ much in subplot one when the gear changes in subplot two.

in Figure 4.13. The amount of force generated for a certain friction coefficient varies very little between the curves at lower slip ratio values. Small errors between the forces from the models will therefore generate a larger change of the friction coefficient which is undesired.

The RLS should not be updated when the normalized forces from both the vehicle and tire model is a certain amount below the friction coefficient:

$$\mu_0 \geq \tau \cdot \mu \quad (4.37)$$

where τ is the percentage of the frictional limit that the normalized force has to exceed. This means that the friction coefficient will be updated rarely during calmer driving sequences, which becomes a trade-off for getting a more stable friction coefficient estimator.

When this restriction due to low forces is applied, another problem is introduced. During a situation where the actual tire/road friction drops rapidly, the maximum forces from the vehicle model will drop proportionally. If the system still believes that tire/road friction is high, the Equation 4.37 will never be true and the friction coefficient will not

be updated within the system. To overcome this, a condition that allows the friction coefficient to be updated when the tire force model is much greater than the vehicle force model, is introduced.

$$F_{tire} \gg F_{vehicle} \quad (4.38)$$

Logically, this should only happen when the friction estimation is too high.

Chapter 5

Results

5.1 Tire/road friction for different driving sessions

The most interesting result of all this work is of course the estimated tire/road friction coefficient. But, how the estimator works with the forces and when it actually estimates the friction is also interesting. Most of the resulting plots consist of two subplots, the estimated friction but also the vehicle force and the tire force. The vehicle force is always calculated but the tire force is only estimated in accordance with Section 4.6.3. When these conditions aren't fulfilled the tire force is set to zero in the plots and the estimator is paused.

To eliminate minor disturbances the combined forces for the two front tires are used rather than splitting it up into two different computations. This means that only one friction coefficient will be estimate rather than one for each tire respectively. It would be possible to calculate the friction coefficient for both sides of the vehicle in order to detect a split- μ situation, but the trade-off would be a less stable estimation when both tires have the same friction to the road. A more stable estimation is prioritized in this report.

5.1.1 Winter tires on asphalt

The algorithm that estimate the friction coefficient was run on the straight line acceleration run, as used in Section 4.5.1 to acquire the tire model parameters. The combined forces from the two front tires can be seen for the two respective force models in Figure 5.1, subplot one. The corresponding friction coefficient can be seen in subplot two.

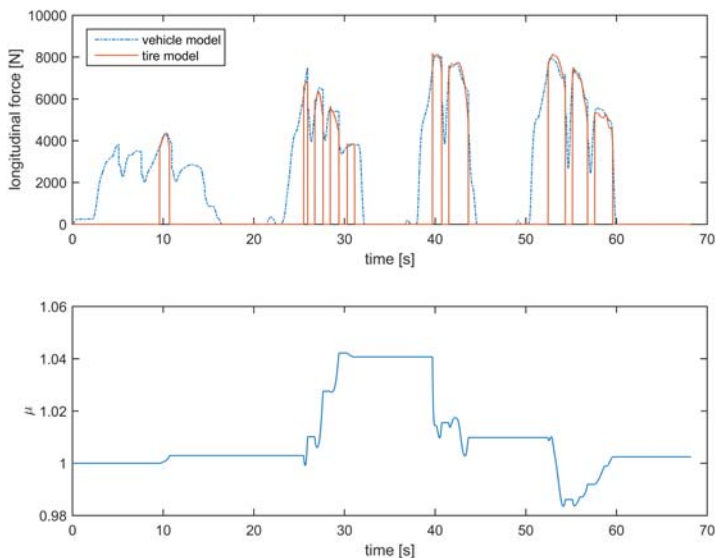


FIGURE 5.1: Force from the tire and vehicle model and the estimated μ for a straight line acceleration.

The friction estimation is seen to be jumpy at certain times, but the changes of frictional value are still quite small. The friction estimation stays around $\mu = 1$, which it evidently should due to the fact that the tire model parameters are fitted during this driving sequence.

A more interesting test for the friction estimation algorithm is a more aggressive driving sequence done at test track. The same tires were used on a similar surface as in the previous driving sequence. The force from the two models and the friction estimation result can be see in Figure 5.2.

The resulting friction coefficient is seen to vary around $\mu = 1$, similar to the straight line acceleration run. In the first subplot, it can be seen that the force from the tire model is calculated quite rarely, meaning that the friction coefficient is only estimated during these moment. However, the resulting μ estimated during these moments are fairly steady around $\mu = 1$.

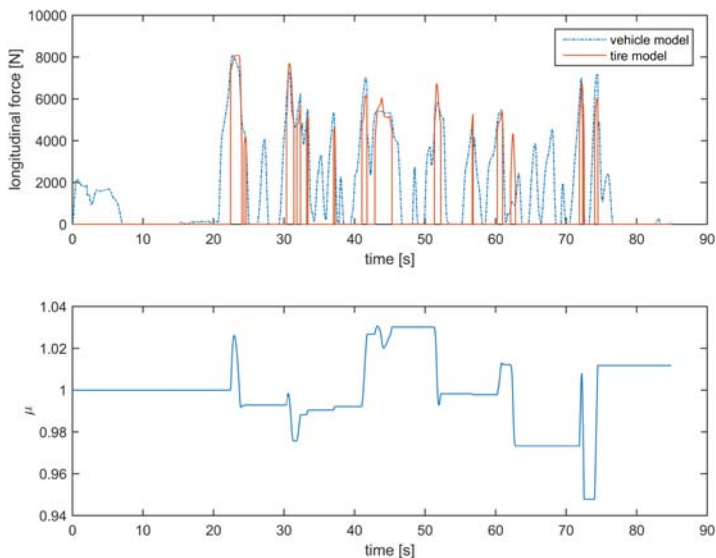


FIGURE 5.2: Force from the tire and vehicle model and the estimated μ for a fast track run.

5.1.2 Winter tires on ice

Being able to detect a surface with a low friction coefficient is probably the most important part of the friction estimation algorithm, due to the risk of an accident if too much torque is transferred to one of the driving axles. The resulting forces from the models and the estimated friction coefficient can be seen for a driving sequence on ice/snow in Figure 5.3.

The winter tire model parameter for low- μ was fitted on this run. It is therefore no coincidence that the friction coefficient end up at around $\mu = 0.4$. It can be seen in the figure that the force calculated from the tire model varies with a higher frequency during the driving sequence on ice/snow compared to the previous sequences. Even though, the resulting friction coefficient is estimated fairly well around friction $\mu = 0.4$, especially when the estimation algorithm is active for a relatively large period of time seen at $t \in [100, 120]$ s. A quite large disturbance of μ can unfortunately be seen at the times $t \in [7, 12]$ s, due to that the vehicle model calculates a higher force than the tire model.

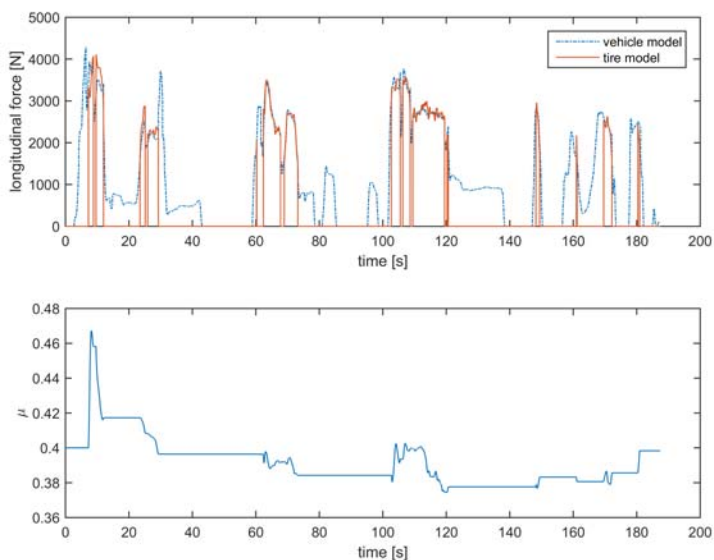


FIGURE 5.3: Force from the tire and vehicle model and the estimated μ for a driving sequence on ice/snow.

5.1.3 Winter tires on asphalt and ice combined

The main goal for the work done in this report was to detect when low- μ is present so that the torque transfer through the FXD can be limited. It is therefore essential to test the developed algorithm during a driving sequence that actually includes a change of μ , preferably from high- μ to low- μ , to verify that the algorithm can handle this kind of abrupt change. It has not been possible to test this on a single run, for example using a driving sequence that includes both asphalt as well as a skid pad. In order to simulate this behavior, two different runs have been merged together, where the friction coefficient changes a total of three times. Starting at high- μ and finishing with low- μ . The merging was made at points where both sequences were accelerating or decelerates at the same velocity, in order to avoid unnecessary jumps of other signals from the vehicle.

The two modeled forces and the resulting μ from the merged run can be seen in Figure 5.4. The estimated friction coefficient is seen to clearly change when a different driving sequences is begun, meaning that the algorithm manages to detect that the grip between the tire and the road differs.

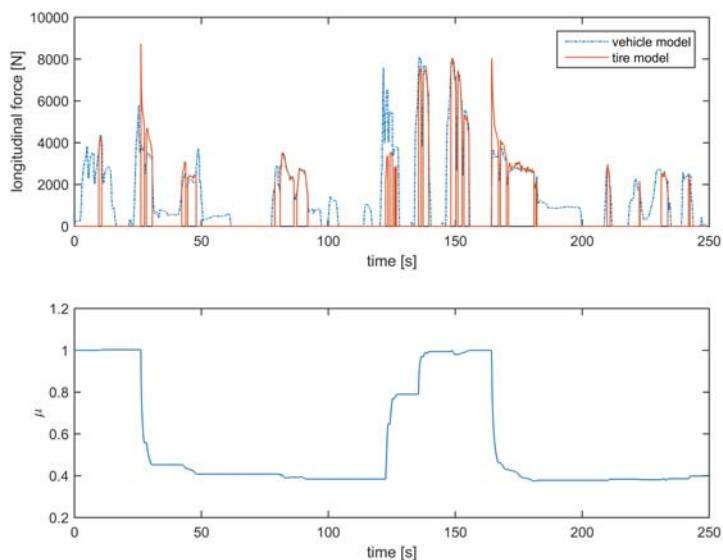


FIGURE 5.4: Force from the tire and vehicle model and the estimated μ for two different runs, with differing μ , merged together (see Figure 5.5 for a detailed view of a sudden friction coefficient drop).

Due to the limitations set concerning when the friction coefficient should be estimated (Section 4.6.3), the algorithm may not update μ at the same instance as the new surface is present. However, when the algorithm is allowed to estimate, the new friction coefficient is estimated with good speed. In Figure 5.5, the two forces and the friction coefficient can be seen when the result is zoomed in on a sudden drop of the friction coefficient. The converging μ is seen to drop very fast as the two forces differs greatly right after $t \approx 26.2$ s, and thereafter decrease more slowly.

The normalized force per slip ratio curve for the combined sequence can be seen in Figure 5.6. Note that this figure is merely the two Figures 4.16 & 4.17 added on top of each other, with some erroneous result due to the wrong calculated force when the friction coefficient suddenly changes. The result clearly shows that a tire's stiffness varies for different surfaces.

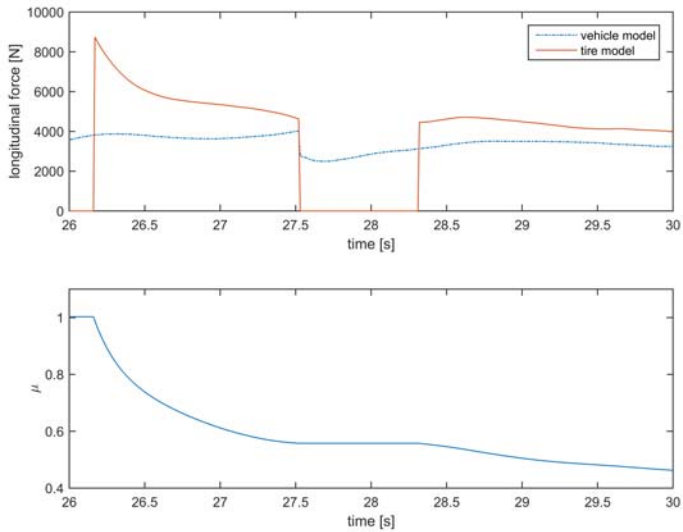


FIGURE 5.5: Zoomed in result of Figure 5.4, showing the speed of the friction coefficient algorithm.

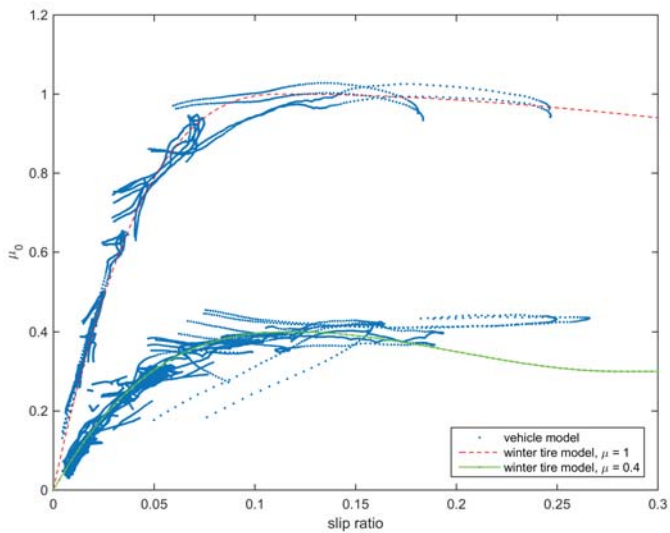


FIGURE 5.6: Force per slip ratio for the combined driving sequence with both low- and high- μ .

5.1.4 Summer tires on asphalt

A fast track lap was also run with the summer tires on asphalt. These tires were, as mentioned before, relatively stiff and with the peak force located at a relative small slip ratio value. This tire attribute makes it tougher to estimate the friction coefficient, due to the fact that variances will result in larger force errors between the two models.

The result from this fast track run can be seen in Figure 5.7. The two first curves, *vehicle model* and *tire model, used value*, are the same calculations as seen earlier in the result, and *tire model, all values* is an additional plot that shows the tire force even when the conditions are not met from Section 4.6.3. The conditions are unfortunately not met at any longer period of times, as the figure shows, even though the forces acting on the vehicle are relatively high at numerous occasions. Hence the curve *tire model, all values* is shown to demonstrate the reasons that the conditions for the friction estimation algorithm are not met.

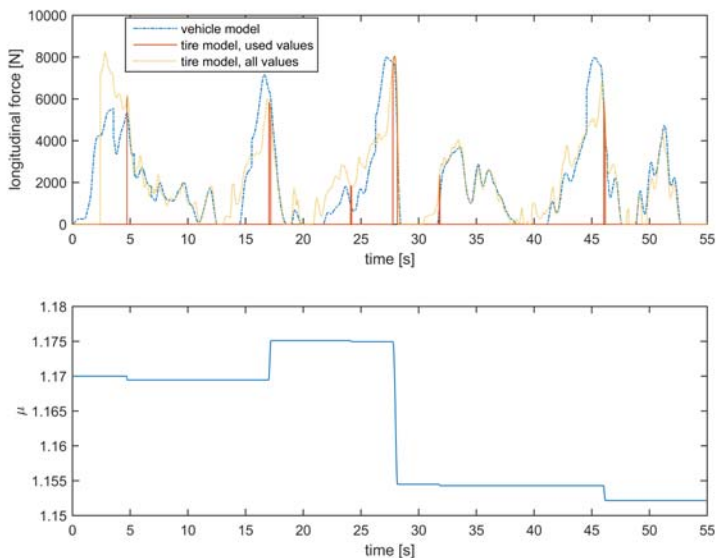


FIGURE 5.7: Force from the tire and vehicle model and the estimated μ for a driving sequence on dry asphalt with summer tires.

5.1.5 Summer tires on wet asphalt

A similar fast track lap was done with the summer tires on wet asphalt, to test the algorithm's behavior on the similar road surface but with different driving conditions. The result from this driving sequence can be seen in Figure 5.8. It can be seen that the resulting μ does not drop much lower than the $\mu = 1.17$ which was calculated during the dry acceleration run.

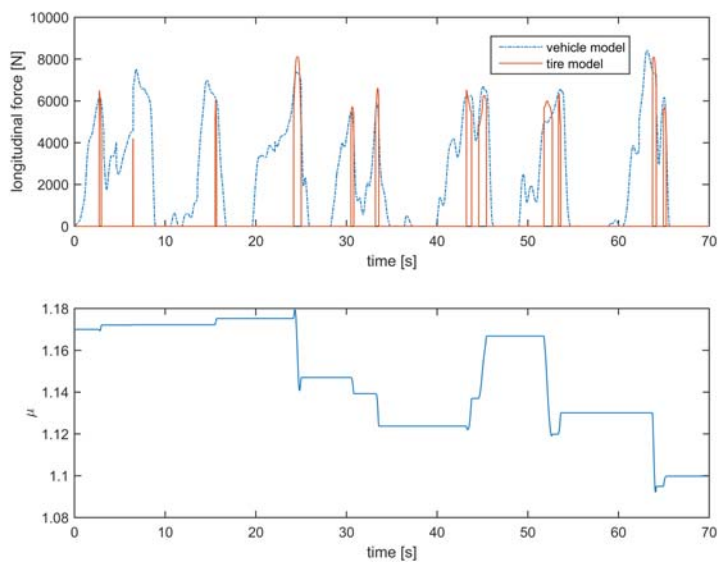


FIGURE 5.8: Force from the tire and vehicle model and the estimated μ for a driving sequence on wet asphalt with summer tires.

The normalized force per slip ratio for the dry and wet acceleration runs respectively are seen in Figure 5.9. The first subplot corresponds to dry asphalt and the second subplot to wet asphalt, where the dashed line in the two subplots are exactly the same tire model parameters. The figure shows that the longitudinal force per slip ratio does not decrease when accelerating is done on wet asphalt.

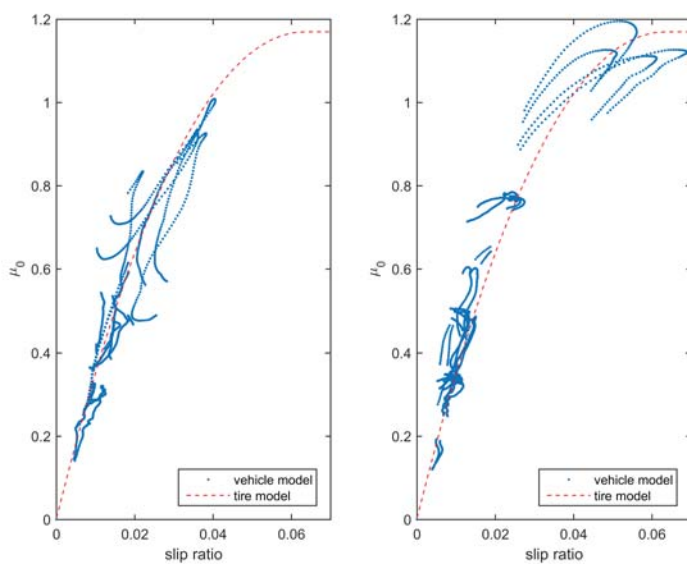


FIGURE 5.9: Normalized force per slip ratio. Subplot one for dry asphalt and subplot two for wet asphalt.

Chapter 6

Discussion

6.1 Modeling the forces

A vehicle and a tire are complex matters and therefore hard to describe with theoretical models. There are many factors that have been simplified and approximated in order to make appropriate calculations. Along the way, these simplifications and approximations do not always agree with reality, which makes the results unreliable.

6.1.1 The complexity of a tire

One of the greatest challenges in this work was to model a tire correctly. Even a normal road tire, nothing fancy at all, is an extremely complex structure to model mathematically. One of the most accurate tire models of today is considered to be Pacejka's Magic Formula [7]. The reason for the accuracy is simply that it's a semi empirical model that's actually not connected to a tire's physical properties at all. It's (extremely) simply put just a customizable polynomial that can be adjusted to fit a tire's force per slip ratio curve very well. This is really good in a laboratory environment for example where one specific tire needs to be modeled for a series of tests. It's also not very intuitive to change the parameters to change the model behavior. Instead of a couple of simple inputs like tire stiffness and normal force the formula requires several parameters which are hard or even impossible to obtain. Needless to say, for a real time application in a vehicle there are better options.

The tire model created by Ola Nockhammar at BorgWarner AB that was used, was much simpler but still not as simple as the Dugoff or Brush models. A positive aspect of a simpler tire model is that it's easier to understand and experiment with. The five input parameters (slip ratio, normal force, tire/road friction coefficient, tire stiffness and

curve inclination factor) are affiliated with the real world in a much simpler way than the Magic Formula is. It was fairly easy to implement it together with the tire mode selector and hence it could be used to model both winter and summer tires without any severe modifications. Another advantage is that it does not include very advanced calculations, making it suitable for real-time use in simple micro controllers.

In the beginning of this work it was believed that the tire stiffness was a static parameter for each tire. After some research it was showed that the tire stiffness actually depends heavily on the tire/road friction coefficient. It was impossible make a tire model behave as a tire on both asphalt and ice with a static tire stiffness. If the tire stiffness was modeled as a simple linear function depending on the friction coefficient the model worked much better. This is partly in agreement with [5] which was an article that was read really early but the idea was discarded because it didn't seem to fit the needs. The method in question is the slip-slope method. The idea is to estimate the tire/road friction coefficient by calculating the slope of the force per slip ratio curve while driving. Looking now at the linear functions for the tire stiffness developed in this thesis, it actually verifies Gustafsson's idea to some degree. The slip slope he describes is essentially the same thing as the linear functions for the tire stiffnesses used in this thesis to improve the tire model.

6.1.2 Approximating the losses

The formula for losses in the drive line where the gear ratio has an impact on the efficiency is certainly interesting. It was found on a private person's own web site. The person in question is named Steven Mason and has worked at the rotational machinery and controls laboratory at University of Virginia. Via e-mail contact it was learned that the formula came from lecture notes of T.C. Scott's course in Automotive Engineering and that he hadn't done any extensive tests of it. The formula works really well and since it did, it was chosen to be used even though the source isn't the best. Before the formula was found it was already shown that higher gear ratio appeared to lower the efficiency in the drive line which also strengthened the belief in the formula.

6.1.3 Slip ratio calculations

The main problem regarding the slip ratio calculations is the approximation of the vehicles velocity. What's needed for a good slip ratio calculation is the wheel's velocity relative the road in the exact same direction as the wheel in pointing. Thus, calculating the slip ratio based on the undriven wheel velocity only works good when driving in a straight line. Turning will make it much harder to calculate the true slip ratio value.

Calculations of the velocity in the pointing direction is hard without for example an optical sensor that actually "reads" the road in real time. The biggest improvement would be to consider the lateral velocity of the vehicle as well. To estimate the lateral velocity was considered to be outside the scope of this work, but there already exist methods that could be used to estimate this. By combining longitudinal and lateral velocity, yaw rate and the wheel angle, the wheel's actual heading velocity relative to the ground could be calculated, enabling a much better slip ratio estimation.

6.1.4 Weight load transfer

The weight transfer that actually affects the vehicle has a high impact on the used normal force for each tire, which has a high impact on the tire model force. The weight transfer function used in this work is rather simplified and a more correct way of calculating has unfortunately not been performed. A more accurate weight transfer model could make the tire force model more accurate.

6.2 Evaluating the results

A further explanation of the results seen in Chapter 5 will be presented in this section. The results are generally not revolutionizing with a quick and stable friction coefficient estimation, but rather show the results of real driving sequences. In some of the driving scenarios the friction coefficient is estimated fairly well, but in some cases the algorithm is shown to be insufficient.

6.2.1 Using winter tires

The results that are presented when using the winter tires are overall better. Both the fast track run, the ice/snow driving sequence and the combined asphalt and ice/snow run show promising results when it comes to actually estimating the friction coefficient. The run done on the fast track with a lot of lateral acceleration (Figure 5.2) shows that the lateral acceleration compensation works quite well.

The result that was seen in Figure 5.3 showed that the tire force varied with high frequency compared to the runs made on asphalt. The reason for this is the attribute of snow. The snow will make the road more bumpy making the wheel speeds, and therefore also the slip ratio, vary more. The snow is also pushed aside as the tires rotate, leading to further uneven signals. Even though these disturbances exist, the forces from the two models match quite good, leading to a fairly stable friction estimation.

During the combined sequence, it is clearly seen that two different friction coefficients between the tire and road are found. Due to the algorithm's updating conditions, this takes a while longer at certain situations. In the zoomed in figure (Figure 5.5), it can be seen that the friction estimation drops to $\mu \approx 0.6$ in under one second, which is two-thirds of the target friction at $\mu = 0.4$. The speed of the convergence is highly dependent on the λ -value chosen for the RLS fitting method. With a choice of a smaller λ , the change of μ would be found faster, but to the price of a less stable estimation which would be more prone to consider errors.

6.2.2 Using summer tires

The outcome from the driving sequence with summer tires on dry asphalt shows some disappointing result. The sequence from a fast track lap is active almost a minute and the modeled forces are high numerous times. Despite this, the algorithm is barely active and the friction coefficient is only updated at a couple of short instances. The third line in Figure 5.7, *tire model, all values*, is plotted to explain why the algorithm never gets the chance to update.

In the beginning of the run, time ≤ 5 s, the tire model is shown to calculate a much higher force than the vehicle model. This is because a steering angle is present at a relatively low velocity, leading to a high slip ratio between the front and rear wheels. It is therefore correct to not update the friction coefficient at this time.

There are three other occasions where the force from the vehicle is high and where the friction coefficient possibly could be estimated. These times are at around 17, 27, and 45 s. What happens at these moments is that the car has geared down, with a so called *kickdown*, when the driver requests a higher acceleration. The result of a kickdown is that the expected force from the vehicle model is much greater, for a short period of time, than it actually is. This difference in force can be seen from the two curves *vehicle model* and *tire model, all values*, at these mentioned times. It is therefore correct to not let the algorithm update the friction coefficient at these times.

If the times mentioned above are excluded, the *vehicle model* and *tire model, all values* match quite well. At around 35 and 50 s, it is seen that the two models reflect each other closely. Unfortunately, the normalized forces are too far from the frictional limit, hence the friction estimation is said to be too inaccurate.

Another interesting result when using the summer tires on both dry and wet asphalt is that the amount of force generated per slip ratio, and therefore also the friction coefficient, seem to differ very little when comparing the two conditions. In Figure 5.9

it can be seen that the normalized force is larger for certain slip ratios when the driving was done on wet asphalt.

Chapter 7

Conclusion

7.1 Model parameters

One of the larger insights acquired was that the difference between tire sets had a much bigger impact than what was expected. It was first believed that most tires had the force peak at similar slip ratio values, but after extensive testing this was found not to be true. Therefore the tire model needed to be extended to handle both different tires and road conditions. However, test driving have only been performed with two different sets of tires which of course restricts the possibilities to create a friction coefficient estimator that works for all tires. It's believed that the tire selector that has been developed can easily be extended to handle all kinds of tires but this requires a lot more test data from test driving with different kinds of tires and road conditions.

The estimator in whole could also be extended with several modules to enable better estimation of the friction coefficient. Methods to estimate V_y (lateral velocity) and α (slip angle) could greatly improve estimation of the vehicle states. This would further on improve the reliability of vehicle and tire models.

7.2 CAN signals used

A goal with this thesis was to use signals that are easily available on most new vehicles of today, rather than using parameters that need new sensors or are hard to approximate. The CAN signals used by the estimator to estimate the tire/road friction coefficient were:

- the four wheel speeds

- engine torque
- lateral acceleration
- current gear
- steering wheel angle
- FXD-moment

Besides this, static parameters associated with the Golf GTi was used which of course can be replaced by the static parameters for another car.

7.3 Final words

The work done in this report has focused as much as possible on having a solution that works in real life situations, rather than having a model that works perfectly during simulated testing. All in all this goal was reached and the developed friction estimator works really well for some driving sequences. Above all it's a great start for future development within this area.

Bibliography

- [1] A. Forsén, S. Nordmark, and E. Wennerström. *Fordonsdynamik*. Fordonsteknik, KTH, 1997 edition, 1997.
- [2] A. Forsén, S. Nordmark, and E. Wennerström. *Fordonsdynamik*. Fordonsteknik, KTH, 1999 edition, 1999.
- [3] R. Rajamani. *Vehicle Dynamics and Control*. Springer Science+Business Media, LLC, 233 Springer Street, New York, NY 10013, USA, 2nd edition, 2012. ISBN 978-1-4614-1433-9.
- [4] M. Hjort, J. Svendenius F. Bruzelius. Validation of a basic combined slip tire model for use in friction estimation applications. *Journal of Automobile Engineering*, 228:1622–1629, November 2014. URL <http://pid.sagepub.com/content/228/13/1622.full.pdf+html>.
- [5] F. Gustafsson. Slip-based tire-road friction estimation. *Automatica*, 33(6): 1087–1099, 1997. URL <http://www.sciencedirect.com/science/article/pii/S0005109897000034>.
- [6] Y. Yasui, W. Tanaka, Y. Muragishi, E. Ono, M. Momiyama, H. Katoh, H. Aizawa, and Y. Imoto. Estimation of lateral grip margin based on self-aligning torque for vehicle dynamics enhancement. March 2004. URL <http://papers.sae.org/2004-01-1070/>.
- [7] Hans B. Pacejka. *Tire and Vehicle Dynamics*. Society of Automotive Engineers, Inc., 400 Commonwealth Drive, Warrendale, PA 15096-0001, 2nd edition, 2006. ISBN 0-7680-1702-5.
- [8] W. Li B. Li, H. Du. A novel cost effective method for vehicle tire-road friction coefficient estimation. *2013 IEEE/ASME International Conference on Advanced Intelligent Mechatronics (AIM)*, (9-12):1528–1533, July 2013. URL http://ieeexplore.ieee.org/xpl/login.jsp?tp=&arnumber=6584312&url=http%3A%2F%2Fieeexplore.ieee.org%2Fxppls%2Fabs_all.jsp%3Farnumber%3D6584312.

-
- [9] E. Pierce. differential free, differential locked. 2006/2009, Accessed: 24th July 2015. URL <http://en.wikipedia.org/wiki/User:Wapcaplet>.
- [10] S. B. Choi M. Choi, J. J. Oh. Linearized recursive least squares methods for real-time identification of tireroad friction coefficient. *IEEE Transactions on Vehicular Technology*, 62(7):2906–2918, September 2013. URL <http://ieeexplore.ieee.org/xpl/articleDetails.jsp?arnumber=6508885>.
- [11] S. Mason. Recommended empirical approximation from conversation with Stephen Mason, formerly of the University of Virginia Rotational Machinery and Controls Laboratory; currently with Johns Hopkins Applied Physics Laboratory. From E-mail conversation, May 2015.

Lund University Department of Automatic Control Box 118 SE-221 00 Lund Sweden		<i>Document name</i> MASTER 'S THESIS	
		<i>Date of issue</i> July 2015	
		<i>Document Number</i> ISRN LUTFD2/TFRT--5985--SE	
<i>Author(s)</i> Simon Johansson Viking Persson		<i>Supervisor</i> Ted Brink, BorgWarner AB Ola Nockhammar, BorgWarner AB Tore Hägglund, Dept. of Automatic Control, Lund University, Sweden Anders Robertsson, Dept. of Automatic Control, Lund University, Sweden (examiner)	
		<i>Sponsoring organization</i>	
<i>Title and subtitle</i> Tire/road friction estimation for front wheel driven vehicle			
<i>Abstract</i> <p>Vehicles of today are equipped with several driving enhancing systems. The Electronic Stability Program (ESP) controls the brakes of the vehicle to prevent undesirable vehicle behavior. The Anti-lock Braking System (ABS) prevents the wheels to lock up while braking hard. Many vehicles are also equipped with advanced All Wheel Drive (AWD) systems or Limited Slip Differentials (LSD) allowing for the drive torque to be almost freely distributed among the wheels. Knowing the coefficient of friction to the road is extremely beneficial for all of these systems, especially for the AWD and LSD systems to be able to optimize the control.</p> <p>In this master thesis a method for estimating the tire/road friction coefficient will be developed. Focus will be put on Front Wheel Driven (FWD) vehicles equipped with an electronic Limited Slip Differential (eLSD). The eLSD in question is a newly launched product by BorgWarner AB called FXD (Front Cross Differential). This is an eLSD based on their well known fifth generation electro hydraulic clutch. Today it's controlled by a complex control algorithm to be able to handle several driving situations. It's desirable to know the tire/road friction coefficient to improve the control algorithm further. This is especially important when estimating the torque transfer through the differential.</p>			
<i>Keywords</i>			
<i>Classification system and/or index terms (if any)</i>			
<i>Supplementary bibliographical information</i>			
<i>ISSN and key title</i> 0280-5316			<i>ISBN</i>
<i>Language</i> English	<i>Number of pages</i> 1-84	<i>Recipient's notes</i>	
<i>Security classification</i>			